博士論文番号：1581203

(Doctoral student number)

The Effect of Cholesterol on the Membrane Shaping by PACSIN2 and Its Implication in Caveolae Formation

Aini Gusmira Amir

Nara Institute of Science and Technology

Graduate School of Biological Science

Molecular Medicine and Cell Biology Laboratory

(Prof. Shiro Suetsugu)

Submitted on 17 September 2019

TABLE OF CONTENTS

Graduate School of Biological Sciences Doctoral Thesis Abstract

Lab name (Supervisor)	Molecular Medicine and Cell Biology (Prof. Shiro Suetsugu)		
Name (surname) (given name)	Amir, Aini Gusmira	Date	2019/08/20
Title	The effect of cholesterol on the membrane shaping by PACSIN2 and its implication in caveolae formation		

The subcellular structures are mostly composed of the lipid membrane, and the remodeling of such lipid membrane is essential for the formation and maintenance of subcellular structures. Several membrane-remodeling proteins are known to impose specific shapes into the membrane. These membrane remodeling proteins include the Bin-Amphiphysin-Rvs (BAR) domain-containing proteins. Among the BAR domain-containing proteins, PACSIN2 (or Syndapin II) is a member of F-BAR (FES-CIP4 homology (FCH)-BAR) domain proteins, a subfamily of BAR domain-containing proteins that are involved mostly in the tubule-like invaginations of the plasma membrane or tubular structure formation of intracellular organelles.

PACSIN2 is localized to the neck of caveolae, membrane invaginations that resemble flask with a diameter of ~100 nm. Caveolae are abundant in endothelial and muscle cells, which are the cells under mechanical stresses. Caveolar membrane invaginations are flattened for the buffering of membrane tension. The membrane shaping ability of PACSIN2 is shown to be essential for caveolar morphogenesis, presumably through the shaping of the caveolar neck. When the cells are treated with hypoosmotic tension, protein kinase C (PKC) phosphorylates PACSIN2 at Serine 313, leading to the removal of PACSIN2 from caveolae, which accompanies the flattening of caveolae upon tension application. The phosphomimetic mutation of PACSIN2 (PACSIN2 S313E) has weaker binding to liposomes made of bovine brain Folch, suggesting the phosphorylation induced by a tension weakens the affinity of PACSIN2 to the membrane.

Preceding studies identified the lipids in caveolar membrane. Caveolar membrane is the lipid bilayer and is composed of phospholipids, which are phosphatidylserine (PS) and phosphatidylcholine (PC). PS and PC have hydrophilic head groups, serine and choline, respectively, as well as two fatty acid tails. These fatty acids are reported to be palmitic acid and oleic acid in caveolae, therefore, the majority of lipids are supposed to be palmitoyl-oleoyl phospholipids. Furthermore, caveolar membrane contains abundant cholesterol, which is essential for caveolar formation because depletion of cholesterol results in the disappearance of flask-shaped caveolae. On the other hand, the tension application onto the membrane flattens caveolae, raising the possibility that tension inhibited the membrane remodeling by the proteins such as PACSIN2. However, it had been unclear whether the membrane remodeling of PACSIN2 with or without phosphorylation is dependent on caveolae-specific lipid composition and the tension applied to the membrane. In this study, membrane remodeling ability of PACSIN2 was examined using liposomes having similar lipid composition as caveolae. The liposomes with or without cholesterol: palmitoyl-oleoyl (PO) PC/POPS and POPC/POPS/Cholesterol were prepared. The binding of PACSIN2 F-BAR to these liposomes was examined by the liposome co-sedimentation assay. The binding of PACSIN2 F-BAR to cholesterol-containing palmitoyl-oleoyl lipid liposomes (POPC/POPS/Cholesterol) was weaker than that to the cholesterol-less liposomes with palmitoyl-oleoyl lipids (POPC/POPS). Therefore, cholesterol was suggested to weaken the binding affinity of PACSIN2 F-BAR to the membrane.

Next, the effect of tension on PACSIN2 F-BAR binding affinity to liposomes was investigated by the tension applied to the liposomal membrane by the hypo-osmotic pressure in a range without membrane rupture. The liposomes without tension were also prepared by using the isotonic buffers. The binding affinity of PACSIN2 F-BAR to liposomes composed of POPC/POPS and POPC/POPS/Cholesterol remained unchanged under tension below the membrane rupture.

To investigate the effect of the phosphorylation of PACSIN2 that occurs upon tension application to the cells in vitro, the phospho-mimetic mutant of PACSIN2 (PACSIN2 S313E) was compared with full-length PACSIN2 for their membrane binding. The binding of PACSIN2 and PACSIN2 S313E to POPC/POPS remained similar. Interestingly, the binding of PACSIN2 S313E mutant to the cholesterol-containing membrane was much weaker than that of PACSIN2. Therefore, the phosphorylation at Serine 313 weakens the PACSIN2 binding to cholesterol-containing membrane, which suggested the cholesterol is required for the removal of PACSIN2 from caveolae upon tension application indirectly through phosphorylation.

The morphology of liposomes was then examined by a transmission electron microscope (TEM). The POPC/POPS/Cholesterol liposomes were deformed by PACSIN2 F-BAR domain into 'the beads on the string' morphology, which might resemble the curvature of the flask-shaped caveolae. In contrast, POPC/POPS liposome without cholesterol was deformed by PACSIN2 F-BAR domain into straight tubules. Therefore, the change in the affinity of PACSIN2 to the membrane might induce the change in morphology that is imposed by PACSIN2. Consistent with the difference in the binding by co-sedimentation assay for these liposomes, there were no significant changes in the liposome morphology upon tension application for liposomes with palmitoyl-oleoyl lipids. Therefore, the affinity of PACSIN2 to the membrane appeared to be correlated with the membrane morphology, which is altered by the presence of cholesterol. Cholesterol in the membrane reduces the membrane remodeling activity of PACSIN2, which appeared to occur independently of tension in this lipid composition.

The ability of cholesterol to modulate PACSIN2 remodeling activity was predicted to occur through the modulation of the hydrophobic loop insertion because the loop is inserted into the space in the bilayer membrane of cholesterol localization. Surprisingly, the presence of cholesterol and of tension did not change the depth of the loop insertion. Therefore, the unchanged depth of loop insertion indicated the similar membrane-binding mode of the membrane-bound PACSIN2, indicating the number of PACSIN2 molecules on the membrane was reduced in the presence of cholesterol, presumably by the decrease in the charge density upon the cholesterol addition.

In conclusion, the membrane binding of PACSIN2 is negatively regulated by cholesterol independent of tension itself. The neck of caveolae is the region where the cholesterol concentration at caveolae starts to decrease. Therefore, PACSIN2 localization at the neck of caveolae is thought to have resulted from the lower binding of PACSIN2 to the cholesterol-containing membrane than the plasma membrane with a lesser amount of cholesterol. The analysis of PACSIN2 localization using the cells with a decrease of plasma membrane cholesterol supported the negative regulation of the membrane binding of PACSIN2 for caveolae maintenance. Therefore PACSIN2 is suggested to remodel the membrane dependent on cholesterol for caveolar morphology.

1. INTRODUCTION

1.1 Membrane curvatures of the subcellular structures

The lipid membrane is one of the essential components of life. The outermost surface of the eukaryote cells is considered to be the plasma membrane. The plasma membrane has various subcellular structures of various functions, including invaginations such as caveolae and clathrin-coated pit, as well as protrusions such as phagocytic cup, filopodia, lamellipodia, and podosome (Suetsugu et al. 2014; Safari and Suetsugu 2012; Buccione et al. 2004) (Fig 1). Several proteins have been known to remodel membrane into these shapes. These proteins are called membrane remodeling proteins (Simunovic et al. 2013; Knævelsrud et al. 2013; Frost et al. 2009). Among them are coat forming proteins including coat protein complex I (COPI), coat protein complex II (COPII), and clathrin, the membrane scaffolding proteins including BAR (Bin/amphiphysin/Rvs) domain proteins and the endosomal sorting complex required for transport (ESCRT), the nucleotide-binding proteins including the dynamin family of proteins and Eps15 homology (EH)-domain containing proteins (EHDs), and the membrane-embedded proteins including caveolin and flotillin (Zimmerberg and Kozlov 2006; Shibata et al. 2009; Suetsugu et al. 2014; Prinz and Hinshaw, 2009).

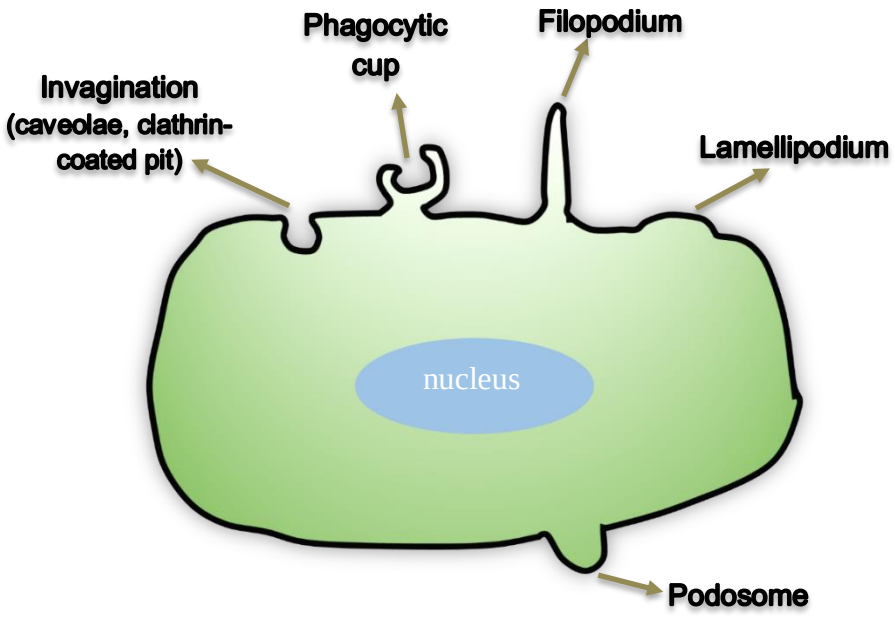

Figure 1: Various cellular membrane shapes

1.2 BAR domain superfamily proteins

Among these proteins with membrane remodeling abilities, the BAR domain proteins function in dynamic membrane remodeling by their characteristic protein structures that are thought to correspond to the membrane curvatures. The first analyzed BAR domain from amphiphysin and many other BAR domains adapt crescent or banana-shaped, and their positively charged lipid-binding surface structure features a concave shape (Peter et al. 2004; Suetsugu et al. 2014; Qualmann et al. 2011) (Fig. 2). The BAR domain proteins can be found in approximately 70 proteins in humans, and classified into several subfamilies dependent on the amino-acid sequence similarity, which are (N-)BAR, F-BAR, and I-BAR subfamilies (Frost et al. 2009; Qualmann et al., 2011; Rao and Haucke 2011; Salzer et al., 2017) (Fig 3). Some members of BAR domain subfamily possess N-terminal amphipathic helices, and thus called N-BAR domain. The amphipathic helices can be hemi-inserted into the membrane, thereby promoting the membrane binding of the BAR domains and the generation of membrane curvatures (Peter et al. 2004; Gallop et al. 2006; Cui et al. 2011). However, most of the BAR domains do not have the membrane insertion motifs (Peter et al. 2004; Carlton et al. 2004; Shimada et al. 2007; Pylypenko et al. 2007), except N-BAR domain and the subset of F-BAR domains of PACSINs/Syndapins (Qualmann et al. 2011; Mim and Unger 2012). Then, the BAR domains bind to the membrane through the electrostatic interactions. All of the BAR domains have their surface enriched in the positively charged amino-acid residues, and the negatively charged membrane lipids including phosphatidylserine (PS) and phosphoinositides interact to these positively charged BAR domain surface, thereby imposing the protein structure to the membrane. Because PS is abundant in the plasma membrane, and the phosphoinositides can be generated upon activation of signal transduction cascade for various biological processes, the BAR domains are supposed to generate and sense membrane curvatures dependent on such negatively charged lipids.

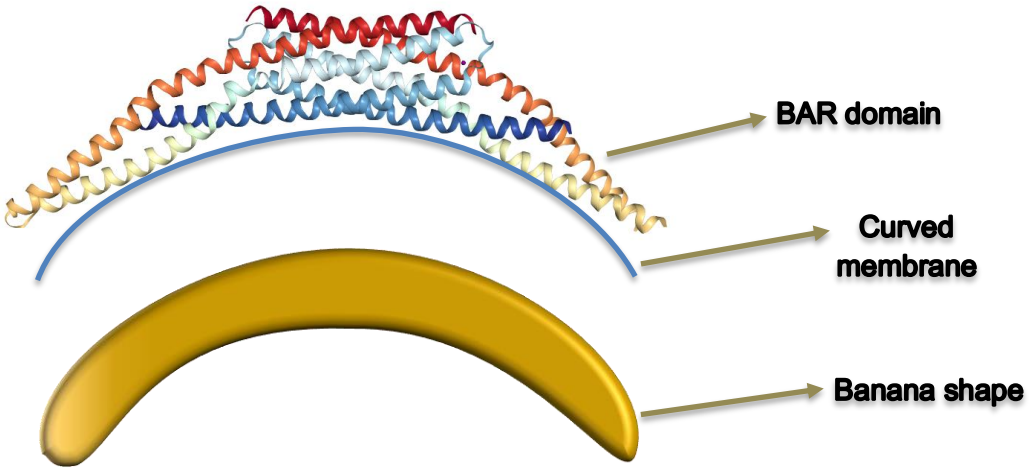

Figure 2: BAR domain from human Bin1/Amphiphysin II that features banana-shape impose its intrinsic curvature on membrane

The (N-)BAR and F-BAR domain proteins sculpt the membrane into invagination by the positive curvature, i.e., concave or banana-shaped curvature of the protein structures, whereas the I-BAR domain proteins generate membrane protrusion by negative curvature of the protein structures (Fig. 3). The structures where the BAR domain proteins functions include the invagination for endocytosis through clathrin-coated pits and caveolae, while protrusions include filopodia and lamellipodia (Suetsugu et al. 2010; Rao and Haucke 2011; Jarsch et al. 2016). These invaginations of the plasma membrane are considered to be reconstituted in vitro because the in vitro tubules of liposomes are generated by the reconstituted protein-free liposomes in the presence of the purified BAR domain proteins. Therefore, the importance of the BAR domain proteins in the shaping of the membrane structures had been strongly accepted (Masuda et al. 2006; Frost et al. 2008; Shimada et al. 2010). Besides invagination, F-BAR domain proteins are also localized to the neck of protrusions (Shimada et al. 2010). The varieties of BAR domains and their structures are supposed to be important for generating various precise curvatures of various membrane structures of the cells (Suetsugu et al. 2010).

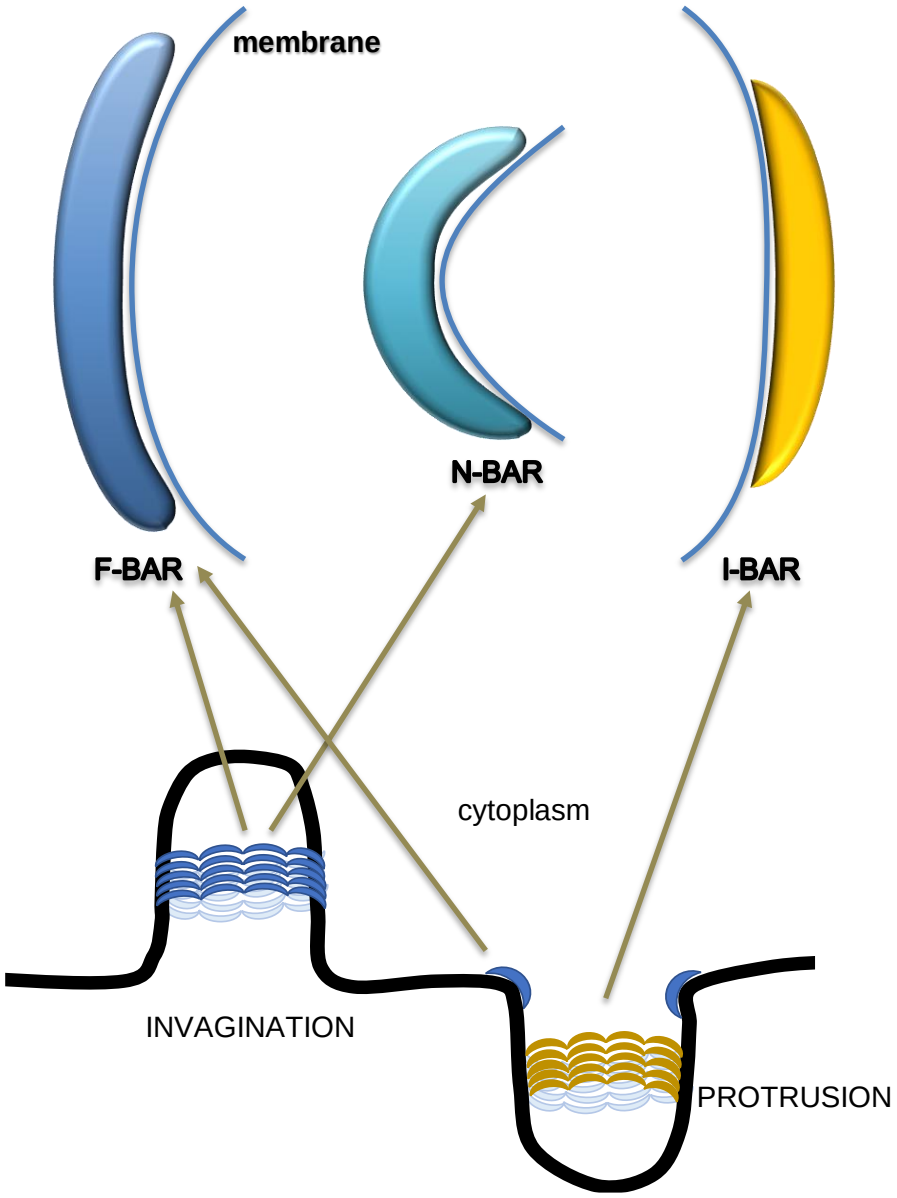

Figure 3: Three types of BAR domain proteins and their localization in the cell membrane. F-BAR and N-BAR produce positive curvature, while I-BAR induces the formation of negative curvature. F-BAR possess shallower curvature compared with deeper curvature of N-BAR. F-BAR and N-BAR are mainly localized at the neck of invagination, while I-BAR is mainly at protrusions.

1.3 Caveolae, cholesterol-dependent plasma membrane invagination for mechanical stress and endocytosis

Caveolae are flask or bulb-shaped invaginations with diameters from 50-100 nm (Fig. 4). Caveolae are abundant in adipocytes, endothelial cells, and muscle cells, which are the cells that undergo mechanical stress or tension during their lifetime, but are absent in neurons, lymphocytes, and kidney proximal tubule (Parton, 2018; Sinha et al., 2011). Caveolae are proposed to function as mechano-sensor and mechano-protector, because when the tension is applied to caveolae, caveolae flatten out by their disassembly, which is thought to buffer the tension applied to the plasma membrane (Parton, 2018; Razani et al., 2002; Sinha et al., 2011) (Fig. 5). Caveolae are also the membrane invagination for endocytosis. Various receptors and channels are known to be localized at caveolae, and are supposed to be internalized into the cells (Pelkmans and Helenius 2002; Frank et al. 2003; Parton 2018). The endocytosed caveolae are sometimes used for transcytosis, the vesicle transport across the cells (Bai et al. 2017; Frank et al. 2009).

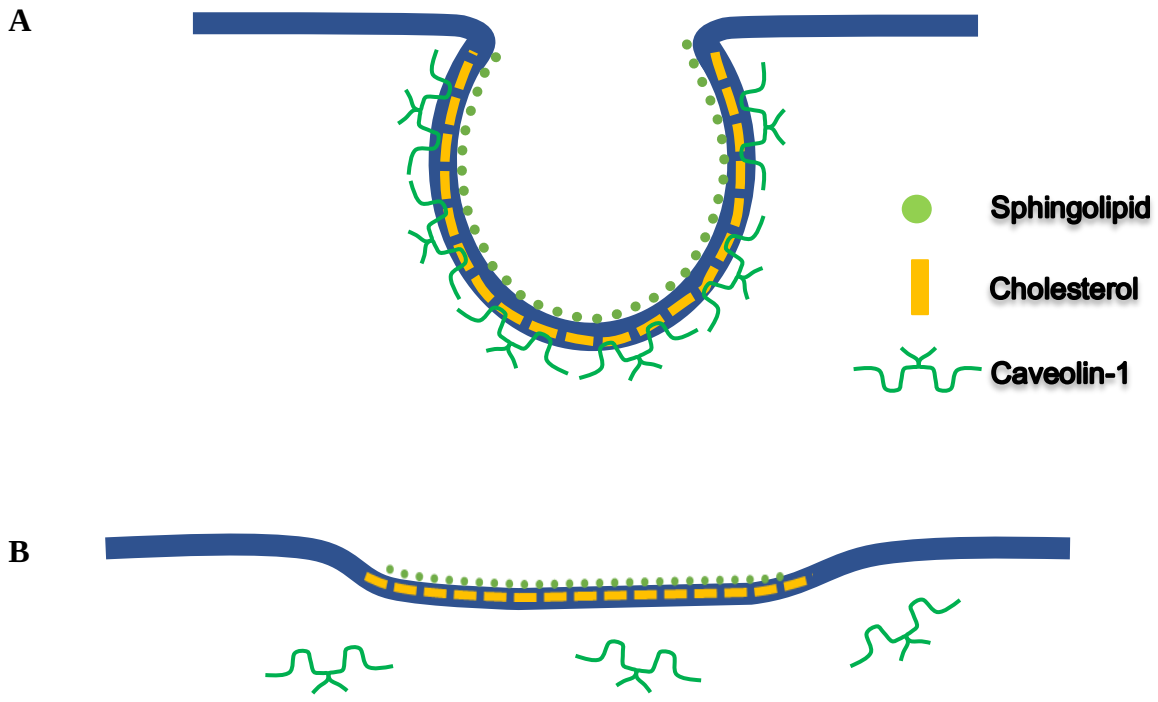

Figure 4: Caveolae membrane. A. Caveolae structure and the main components. B. Impaired caveolae due to cholesterol depletion.

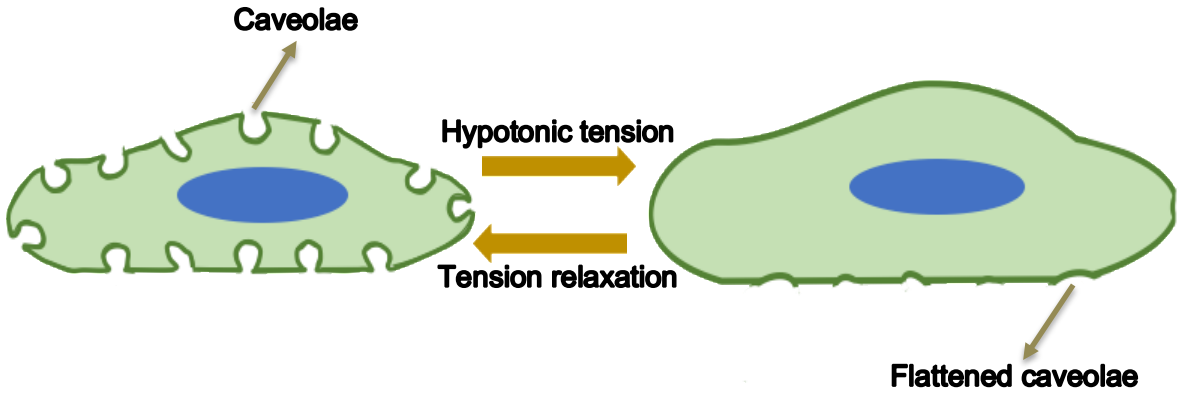

Figure 5: Cell with abundant caveolae at the membrane surface. Cell resist hypotonic tension by expanding its surface twofold through caveolae flattening and caveolae reassemble upon tension relaxation.

The membrane of caveolae is composed of several types of lipids. Caveolae are enriched in cholesterol at both leaflet and sphingolipids at their outer leaflet. Cholesterol is highly enriched in caveolae (Ortegren et al., 2004; Razani et al., 2002; Smart et al., 1999). Up to 41% of membrane lipids of caveolae in adipocytes was reported to be cholesterol, which is very high cholesterol content because the typical amount of cholesterol outside caveolae is approximately 22% (Ortegren et al. 2004). Furthermore, cholesterol is an essential component of caveolae, because cholesterol depletion impairs the morphology of caveolae (Fig. 5) (Breen et al., 2012; Dreja et al., 2002; Parpal et al., 2001; Razani et al. 2002). In such an enrichment of cholesterol, caveolae are considered to be special subsets of lipid rafts marked by caveolin proteins (Patel and Insel 2009; Pike 2003; Razani et al. 2002). The phospholipids that compose the plasma membrane are phosphatidylserine (PS), phosphatidylcholine (PC), phosphatidylethanolamine (PE), and phosphatidylinositol (PI). In caveolae, PC is the major phospholipids (Pike et al., 2005; Smart et al., 1999). PS is also shown to be abundant in the cytoplasmic leaflet of caveolae (Fairn et al., 2011; Pike et al., 2005). The depletion of PS was shown to result in the loss of caveolae morphology (Hirama et al., 2017). The main fatty acids of caveolar phospholipids are oleic acid (C18:1), palmitic acid (C16:0) (Cai et al., 2013; Huot et al., 2010), and stearic acid (C18:0) (Cai et al., 2013). Palmitic acid and stearic acid are predominant fatty acids that bind caveolin-1 (Cai et al., 2013). 16:0-18:1 PC and 16:0-18:1 PS are abundant phosphatidylcholine and phosphatidylserine in the caveolar membrane (Pike et al., 2005).

The essential structural protein is caveolin. Caveolin interacts with cholesterol (Murata et al. 1995), and a caveola contains approximately 150 caveolin proteins (Pelkmans and Zerial 2005), explaining the reason for the enrichment of cholesterol in caveolae. There are caveolin-1, caveolin-2, and caveolin-3. Caveolin-1 and caveolin-3 are the essential protein for caveolar formation (Tachikawa et al. 2017; Jung et al. 2018; Kovtun et al. 2015; Parton 2018). Caveolin-1 is ubiquitously expressed, but the expression of caveolin-3 is limited to muscles (Park et al. 2002; Williams and Lisanti 2004). The knockout of caveolin-1 or caveolin-3 is reported to result in the loss of caveolae. Although the defects by caveolin-1 knockout are limited in endothelial cells and fibroblasts, such as pulmonary fibrosis, hypertension or cardiac hypertrophy, (Zhao et al. 2002; Le Lay and Kurzchalia 2005), the knockout or dysfunction of caveolin-3 resulted in the abnormality in muscles. There are a lot of caveolin-3 mutations that are associated with muscular dystrophies and cardiomyopathies (Parton 2018), that exhibits the fragile muscle without tolerance to stretches (Dewulf et al. 2019). Such disease-associated mutations of caveolin-3 support the essential role of caveolar for tension buffering of the cells.

1.4 The essential roles of PACSINs/Syndapins for formation and maintenance of caveolae

PACSINs (also known as syndapins) are F-BAR domain protein members that are localized to invaginations such as endocytic sites including caveolae and interact with endocytic proteins. PACSINs contain an F-BAR domain at their N-terminus and the Src homology 3 (SH3) domain at the C terminus that interacts with dynamins and Wiskott-Aldrich syndrome protein (WASP) proteins (Kessels and Qualmann, 2004; Modregger et al., 2000; Shimada et al. 2010). The structural analysis of PACSIN1 and PACSIN2 F-BAR domains revealed that the F-BAR domains have the positively charged concave surface analogously as the other BAR and F-BAR domains for the electrostatic interaction with negatively charged lipids including PS on their concave side for the membrane invaginations. The F-BAR domains of PACSINs have their specific hydrophobic loops that protrude on the concave membrane-binding surface of the structure, which are inserted into the hydrophobic region of the membrane that are occupied by cholesterol and the fatty acids of the phospholipids (Shimada et al. 2010; Rao et al. 2010) (Fig. 6). The concave curvature of the F-BAR domain structures of PACSINs is steeper than that of the F-BAR domains that are involved in

clathrin-mediated endocytosis including FBP17 and CIP4, suggesting the involvement of PACSINs in the narrower invagination of the plasma membrane including caveolae.

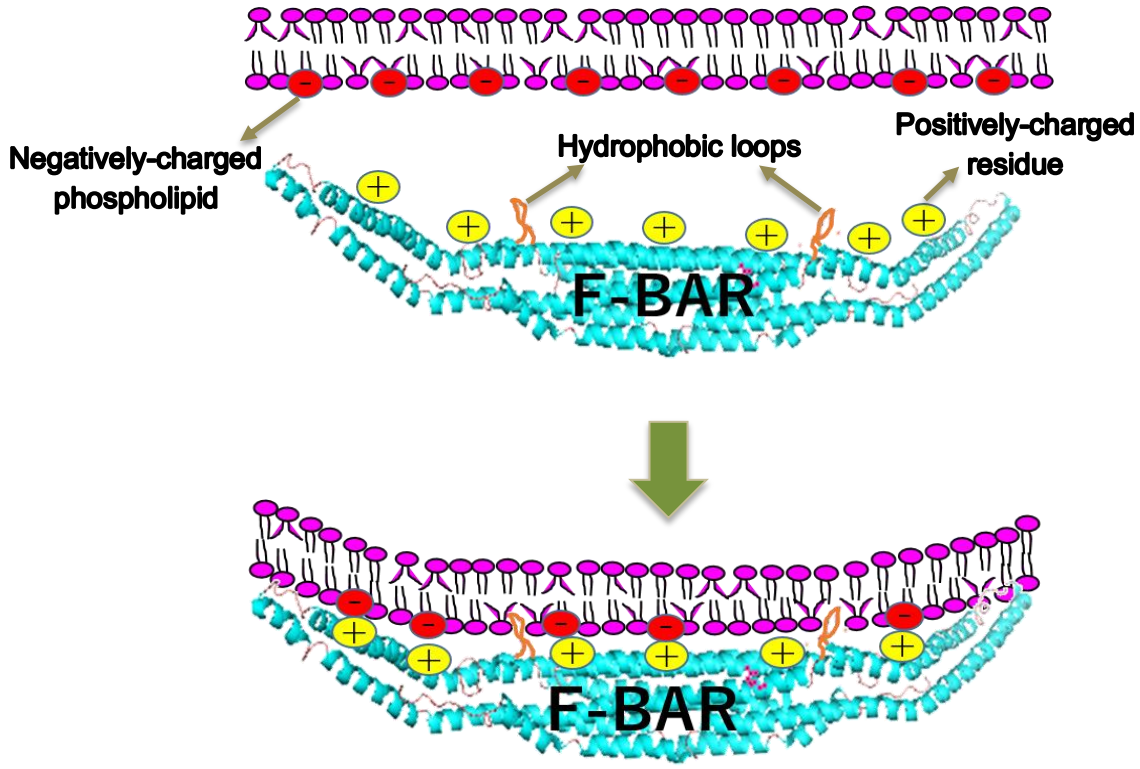

Figure 6: Mechanism of PACSIN2 F-BAR binds cell membrane.

PACSIN isoforms include PACSIN1/syndapin I, PACSIN2/syndapin II, and PACSIN3/syndapin III (Qualmann and Kelly 2000; Wang et al. 2009). PACSIN2 and PACSIN3 have been reported to localized to the neck of caveolae (Hansen et al. 2011; Senju et al. 2011; Seemann et al. 2017). PACSIN3 expression is limited to muscle tissues, while PACSIN2 is ubiquitously expressed. PACSIN1 is neuronal protein, however, its localization at caveolae is unclear (Modregger et al., 2000; Seemann et al., 2017; Senju et al., 2011). PACSIN2 and PACSIN3 are localized at the neck of caveolae, and suggested to interact with caveolin-1 through their F-BAR domain, while PACSIN1 has weak caveolar localization and weak binding affinity to

caveolin-1 (Senju et al. 2011). Interestingly, PACSIN2 and PACSIN3 share some conserved amino acid residues in the F-BAR domains, but these residues are absent in PACSIN1 F-BAR domain. Knockdown of PACSIN2 in HeLa cells impaired the morphology of caveolin-1 associated membranes and reduces the abundance of caveolae (Senju et al., 2011, Hansen et al., 2011; Senju and Suetsugu 2015). Importantly, PACSIN3 knockout mice lead to a loss of muscle plasma membrane invaginations with caveolar morphology, which resulted in the phenotype similar to muscular dystrophy (Seemann et al., 2017). Therefore, PACSINs are thought to play essential role in caveolar morphogenesis.

Upon tension application, PACSIN2 is removed from caveolae by the protein kinase C (PKC) mediated phosphorylation of PACSIN2 at serine 313 (S313) (Senju et al. 2015), which is supposed to be mimicked by the substitution of the serine 313 amino-acid residue to glutamate, which resulted in the S313E mutant. The tension applied to the cells by the hypo-osmotic buffer activated PKC, which was demonstrated by the pharmacological inhibitor of PKC (Chou et al. 1998; Davenport et al. 1995; Hermoso et al. 2004; Liu et al. 2003). The PKC-phosphorylated PACSIN2 has a slightly weaker affinity to the liposomes made of the total lipid fraction of bovine brain, which has been widely used for the studies of BAR domains. The weaker affinity of phosphorylated PACSIN2 was supposed to be reasonable because the membrane binding of PACSIN2 is mediated by the electrostatic interaction between the positively charged protein and the negatively charged membrane, where phosphorylation of the protein reduces the amount of positive charge. In cells, the hypo-osmotic treatment reduced the PACSIN2 localization at caveolae (Senju et al. 2015; Senju and Suetsugu 2015). Combined with the reduced binding of the phosphorylated PACSIN2 to the brain Folch liposomes, it was suggested that the phosphorylated PACSIN2 could be removed from caveolae by the weaker affinity of phosphorylated PACSIN2 compared to the non-phosphorylated PACSIN2 upon tension application, leading to the instability of caveolar for the caveolar flattening (Fig. 7) (Senju and Suetsugu, 2015; Senju et al., 2015).

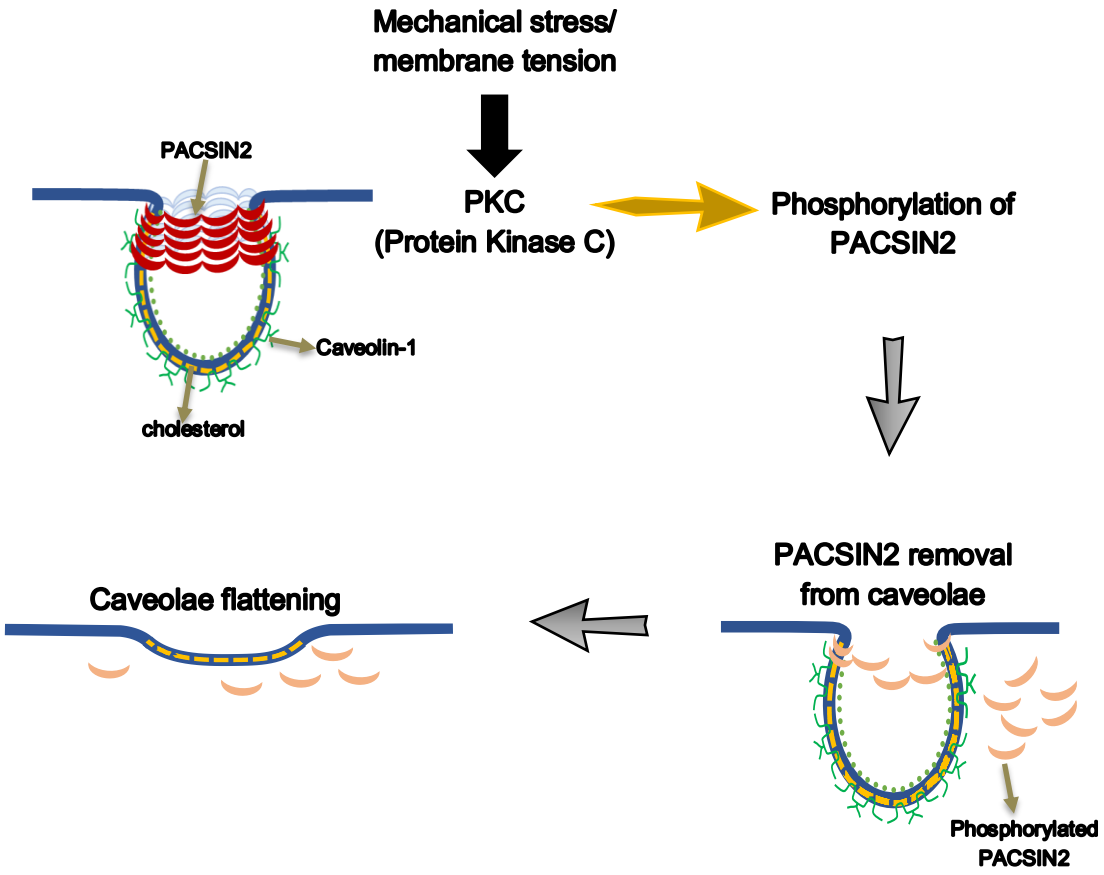

Figure 7: PACSIN2 localizes at the neck of caveolae. Under membrane tension, protein kinase C (PKC) is activated and phosphorylate PACSIN2 at Serine 313, leading to removal PACSIN2 from caveolae and subsequently caveolae flatten out.

1.5 The aim of this study

The above studies showed that PACSINs bind to membrane through its F-BAR domains but did not consider the lipids characteristic to caveolae. The cholesterol was not abundant in the membrane used for the in vitro assays and the tension was not applied to the membranes in vitro. The formation of tubular membrane structure appeared to be opposed by the tension applied to the membrane. Therefore, in this study, I tried to directly examine the role of cholesterol and the tension for the membrane binding of PACSIN2, using its F-BAR domain fragment, full-length protein, and its phosphomimetic S313E mutant. I examined the effect of cholesterol on PACSIN2 F-BAR binding affinity and membrane shaping in vitro reconstituted membrane, i.e., liposomes,

composed of phospholipids with specific fatty acids abundant in caveolae, that were cholesterol and 1-palmitoyl-2-oleoyl PC and PS lipids (POPC and POPS), in the presence or absence of the membrane tension that are induced by hypo-osmolality. I found that cholesterol reduced the affinity of PACSIN2 F-BAR to the liposomes, inhibiting the formation of straight tubules. In contrast, PACSIN2 F-BAR remodeled cholesterol-containing liposomes into 'the beads on the string' formation whose size resemble the size of caveolae (~100 nm). The higher binding affinity of PACSIN2 F-BAR in the absence of cholesterol was correlated with the increased tubular structure formation of PACSIN2 localization upon depletion of cholesterol from the plasma membrane. Importantly, the insertion depth of the wedge loop to the membrane was not altered by the presence of cholesterol. Therefore, the decreased affinity to the cholesterol-containing membrane was the result of the reduced amount of the protein on the membrane, not the alteration of the binding mode of PACSIN2 to the membrane, rather the decrease in the charge density by the inclusion of cholesterol. The phosphomimetic S313E mutant exhibited smaller affinity to the cholesterol-containing liposomes than to the liposomes without the cholesterols, supporting the previous idea of the phosphorylation-induced reduction of the PACSIN2 membrane binding to the membrane. Surprisingly, the tension-applied liposomes within the range without the tension-induced rupture exhibited similar affinity to PACSIN2. These results suggested that the role of PACSIN2 as cholesterol-dependent membrane shaping protein, of which ability to generate membrane tubules were negatively regulated by the caveolar-enriched cholesterol. Consistently, the depletion of cholesterol from the plasma membrane resulted in the enhanced tubules of PACSIN2 with caveolin-1, which were thought to be the intermediates of the caveolar removal from the plasma membrane presumably through caveolar endocytosis. Therefore, this study provides the new role of PACSIN2 for removing the cholesterol-less caveolae from the plasma membrane, which will be important for the maintenance of the cholesterol-enriched caveolae on the plasma membrane.

2. MATERIALS AND METHODS

2.1 Plasmid construction

Mouse PACSIN2 F-BAR (aa 1-305), PACSIN2-mcherry, and PACSIN2 S313E-mcherry were subcloned into pGEX6P1 plasmid by Gibson Assembly® method. Site-directed mutagenesis in PACSIN2 F-BAR M124W was generated by PCR using PrimeSTAR® Max DNA Polymerase, according to the manufacturer's instruction. The plasmids were then transformed into Rosetta Gami B cells by heat shock. The proteins expressed with this method are Glutathione S-transferase (GST)-tagged proteins.

2.2 GST-tagged Protein Purification

Rosetta Gami B containing pGEX6P1-related constructs were cultured in LB medium overnight at 20^{o}C after the IPTG addition. GST-tagged expressed proteins were purified by using GST beads (Glutathione Sepharose 4B, GE Healthcare Life Science). On the next day, cells were pelleted and stored in -80^{o}C as the stocks. Before purification, GST beads were washed with *E.Coli* sonication buffer (10mM Tris HCl pH 7.5, 150 mM NaCl, 1 mM EDTA, 0.5% Triton X-100, Mili Q water) three times. To purify the proteins, cell pellets were resuspended in the mixture of the sonication buffer, 0.1% DTT and 1% PMSF, followed by sonication in an ice container to disrupt the cell membrane (3-sec burst - 3-sec rest for total time 4 minutes). Lysates were then centrifuged at 15,000 rpm for 10 min at 4^{o}C. The supernatant was transferred into GST beads suspension and rotated for 1 hour at 4^{o}C. Then, the beads were centrifuged at 500g for 5 min at 4^{o}C, then the supernatant was discarded, followed by the suspension of the beads in the wash buffer (10mM Tris HCl pH 7.5, 150 mM NaCl, 1 mM EDTA, Mili Q water). This beads washing was repeated more than three times. Subsequently, PreScission Protease (GE Healthcare) was added to remove GST from the proteins, followed by overnight rotation at 4^{o}C. The protein was then separated from GST beads by using minicolumn, then stored as stock in -80^{o}C. The purified proteins were visualized by SDS gel followed by the Coomassie Brilliant Blue (CBB) staining. The concentration of protein was determined by the band intensities of the gels by Image J.

2.3 Osmolality measurement

The buffers osmolality were measured using Wescor Vapro 5600 vapor pressure osmometer, according to manufacturer's protocol. The unit of measurement is mOsmol/kg.

2.4 Osmotically-induced leakage assay

The lipids used in these experiments are porcine brain Folch, 1-palmitoyl-2-oleoyl-sn-glycero-3-phosphocholine (POPC), 1-palmitoyl-2-oleoyl-sn-glycero-3-phospho-L-serine (POPS) dissolved in chloroform, 1,2-dioleoyl-sn-glycero-3-phosphocholine (DOPC), and 1,2-dioleoyl-sn-glycero-3-phospho-L-serine (DOPS) (Avanti Polar Lipids). These lipids were dried under nitrogen gas, then further drying in vacuum for 20 min. The dried lipids were suspended in 300 µl of the Carboxyfluorescein (CF)-NaCl buffer, which contained the indicated concentrations of NaCl, 10mM Tris HCl pH 7.5, 1 mM EDTA, 20 µM 5(6)-Carboxyfluorescein, for 1-2 hr. The osmolarity inside and outside liposomes was adjusted by the NaCl concentration in the CF-NaCl buffer. Alternatively, the dried lipids were solubilized in the Carboxyfluorescein (CF)-sucrose buffer containing 460 mM sucrose, 10mM Tris HCl pH 7.5, 1 mM EDTA, and 40 µM CF. 10 mL of Sephadex G-50 was suspended in the NaCl buffer with the same concentration as NaCl buffer for liposome preparation. Alternatively, Sephadex G-50 was suspended in the glucose buffer containing 460 mM glucose, 10mM Tris HCl pH 7.5, 1 mM EDTA. Sephadex G-50 suspension was then settled in a chromatography column. Then, the liposomes were added to the column and the CF outside of the liposomes were removed. The eluate drops were collected in Eppendorf tubes until CF phase came out. The tubes containing liposomes loaded with CF were confirmed under UV light. These liposomes were then collected in one Eppendorf tubes and divided into three treatment groups; isotonic, hypotonic, and the liposomes for the determination of total CF. All groups were centrifuged at 50,000 rpm for 20 min, and the supernatant was removed. The pellet of the first group was resuspended with isotonic NaCl or Glucose buffer, while the second group was with hypotonic buffer. Both groups were incubated at room temperature for 20 min, followed by centrifugation at 50,000 rpm for 20 min. The fluorescence intensity of the supernatant was measured by spectrofluorometer (Jasco FP-6500). The third group was resuspended with the sonication buffer (10mM Tris HCl pH 7.5, 150 mM NaCl, 1 mM EDTA, 0.5% Triton X-100, Mili Q water) for at least 10 min to release the CF from liposomes. The fluorescence intensity of CF

was measured as the percentage of the total CF. Total CF leakage from liposome was calculated by the following formula:

$$\text{Leakage (\%)} = 100 \times \frac{(F_{hypo} - F_{iso})}{(F_{total} - F_{iso})}$$

where $F_{hypo,}$ F_{iso}, F_{total} are the CF intensity of hypotonic, isotonic, and total CF in liposomes, respectively.

2.5 Liposome preparation for liposomes co-sedimentation assay, Laurdan assay, and Transmission Electron Microscopy (TEM)

Various liposomes were made from 1-palmitoyl-2-oleoyl-sn-glycero-3-phosphocholine (POPC), 1-palmitoyl-2-oleoyl-sn-glycero-3-phospho-L-serine (POPS), 1,2-dipalmitoyl-sn-glycero-3-phosphocholine (DPPC), 1,2-dipalmitoyl-sn-glycero-3-phospho-L-serine (DPPS), cholesterol. These lipids were purchased from Avanti polar lipids. To make liposomes, lipids were dried under nitrogen gas followed by further drying in vacuum for at least 1 hr to remove the traces of residual solvent. 435 mOsmol/kg sucrose buffer (435mM sucrose, 10 mM Tris HCl pH 7.5, 1 mM EDTA, Mili Q water) was then added to the thin layer of dried lipids followed by vortexing to induce the formation of liposomes. The liposome suspension was subjected to ten freeze-thaw cycles of freezing in liquid nitrogen followed by thawing in water bath at 45^{o}C, and then stored in -30^{o}C or immediately used in the assay. Before using, liposomes were extruded through polycarbonate membrane with pore size of 2µm. All liposomes contain laurdan with lipids:laurdan molar ratio of 1:1300.

2.6 Laurdan Assay

Laurdan probe, purchased from Chemodex, was diluted in chloroform before use. After the freeze-thaw cycle, liposomes were extruded through 100 nm pore. To adjust the osmolarity outside liposomes, the liposomes were treated with 435 mOsmol/kg glucose buffer to obtain isotonic

condition (435 mOsmol/kg inside and outside liposome) or with 300 mOsmol/kg glucose buffer to obtain hypotonic condition (435 mOsmol/kg inside and 300 mOsmol/kg outside liposome). Laurdan fluorescence was measured by spectrofluorometer (Jasco FP-6500). The emissions of laurdan were then quantified by calculating generalized polarization (GP) value as bellow:

$$\text{GP value} = \frac{I_{440} - I_{475}}{I_{440} - I_{475}}$$

I_{440} and I_{475} are the emission intensities of laurdan at 440nm and 475 nm, respectively. In general, the higher the GP values, the tighter the lipid packing.

2.7 Liposome Co-Sedimentation Assay

Liposomes used in this assay were composed of POPC/POPS, POPC/POPS/cholesterol, DPPC/DPPS, and DPPC/DPPS/cholesterol. Proteins were mixed with the liposomes. The osmolarity outside liposomes was adjusted by glucose buffer (glucose, 10 mM Tris HCl pH 7.5, 1 mM EDTA, Mili Q water) to obtain isotonic condition (435 mOsmol/kg inside and outside liposome) and hypotonic condition (435 mOsmol/kg inside and 300 mOsmol/kg outside liposome). The mixture was then incubated at room temperature for 20 min, followed by centrifugation at 50,000 for 20 min at 25^{o}C in a TLA100 rotor (Beckman Coulter). The bound proteins were thought to found in the pellet, while the unbound ones were in the supernatant. The pellet and supernatant were then separated, subjected to SDS PAGE and stained by Coomassie Blue Staining (CBB) staining.

2.8 Transmission Electron Microscopy (TEM)

Proteins and liposomes were prepared and mixed as in liposome co-sedimentation assay, and placed on parafilm surface on a heating block set at 25^{o}C. After incubation for 20 min, samples were placed on a grid (Nisshin EM) covered with Polyvinyl Formal (Formvar; Nisshin EM). The NaCl was removed by HEPES buffer. Samples were stained with 0.5% uranyl acetate and air-dried

for several hours to remove the remaining solutions. Dried sections were then observed by transmission electron microscope (Hitachi H-7100).

2.9 Depth of the hydrophobic loop insertion measurement

Quenching of tryptophan (Trp) by brominated phospholipids (Br_2-PCs) was introduced to assess the localization of this residue in bilayers. Liposomes were prepared in several groups: liposomes without quenchers, liposomes with several concentration levels of shallower quencher (6,7 Br_2), and liposomes with several concentration levels of deeper quencher (9,10 Br_2). PACSIN2 F-BAR M124W (5μM) was added to the liposomes solution (0.125 μg/μl) and incubated for 20 min followed by measuring the Trp fluorescence intensity by spectrofluorometer (Jasco FP-6500). The differences in the quenching Trp fluorescence by (6,7) - and (9,10)- Br_2-PC were used to calculate the depth of insertion in the membrane using parallax method (Chattopadhyay and London 1987) as follows

$$Z_{CF} = L_{C1} + [- \ln(F_1/F_2)/\pi C - L_2]/2L$$

where L_{C1} represents the distance from the bilayer center to the shallow quencher (11 Å for 6,7-Br_2-PC), C is the mole fraction of the quencher divided by the lipid area (70 $Å^2$), F_1 and F_2 are the relative fluorescence intensities of the shallow (6,7-Br_2-PC) and deep (9,10-Br_2-PC) quenchers, respectively, and L is the difference in the depth of the two quenchers (0.9 Å per CH_2 or CBr_2 group). For these brominated lipids, the thickness of the hydrophobic region is ∼29 Å.

2.10 Cell culture

HeLa cells were cultured in Dulbecco's modified Eagle medium (DMEM) (Nacalai) supplemented with 10% fetal calf serum (FCS), penicillin, and streptomycin (Meiji pharmaceuticals).

2.11 Transfection

EGFP-labeled PACSIN2 in pEGFP-C1 (Senju et al., 2015) was transfected with the Lipofectamine 3000 and PLUS reagents (Invitrogen), according to the manufacturer's instructions.

mCherry labeled PACSIN2 was prepared by subcloning PACSIN2 cDNA into pmCherry-C1 vectors (Clontech), in which the GFP in pEGFP-C1 was replaced with mCherry. The cells stably expressing caveolin-1-EGFP was prepared as described (Senju et al., 2015). The stable expression of PACSIN2-mCherry was subcloned into pMXs vector, and then was transferred into cells by the retrovirus produced in the packaging cell line Plat-A (Kitamura et al., 2003). After FACS sorting and cloning of the cells, the cells with PACSIN2-mCherry expression equivalent to the endogenous PACSIN2 level were selected by Western blotting for observation.

2.12 Live observation

For live observation by total internal reflection microscopy, HeLa cells were grown on a glass-bottomed dish, with DMEM containing 10% FBS and 10 mM HEPES (pH 7.5). The images were acquired for 5 min at 1 or 0.5 s intervals with a total-internal-reflection (TIRF) microscopy system connected to a confocal microscope (Olympus FV1000D), with a 100× NA 1.45 oil immersion objective (Olympus). The live cells are treated with 10 mM methyl-β-cyclodextrin (MβCD).

3. RESULTS

3.1 Liposomes can resist hypotonic tension up to 160 mOsmol

In the previous study, PACSIN2 was found to be involved in caveolae, which responded to membrane stress by hypotonic tension (Senju et al., 2015), where PACSIN2 was removed from caveolae upon hypoosmotic treatment of the cells (Senju and Suetsugu, 2015). However, the response was not investigated in the reconstituted membrane.

Using hypo-osmotic tension, I examined the effect of tension on the binding and remodeling activity of PACSIN2 F-BAR to liposomes. Osmotic pressure induces the stretching of liposomes, which eventually causes liposomes swelling and rupture (Alam Shibly et al., 2016; Finkelstein et al., 1986). I determined the tension limit that liposomes could exist without rupture by the leakage of the fluorescent molecules from the liposomes (Fig. 8). The liposomes were made with the buffer containing fluorescent molecule, carboxyfluorescein (CF), and then purified using the gel filtration and centrifugation to remove the CF outside of liposomes. Then, the liposomes were treated with a hypotonic buffer to induce tension at the membrane of liposomes. High hypotonic tension can cause liposomes rupture followed by leakage of the internal CF, which are measured by spectro-fluorometer. CF is released from liposomes and relieves the tension when rupture occurs (Hamai et al., 2007; Shoemaker and Vanderlick, 2002).

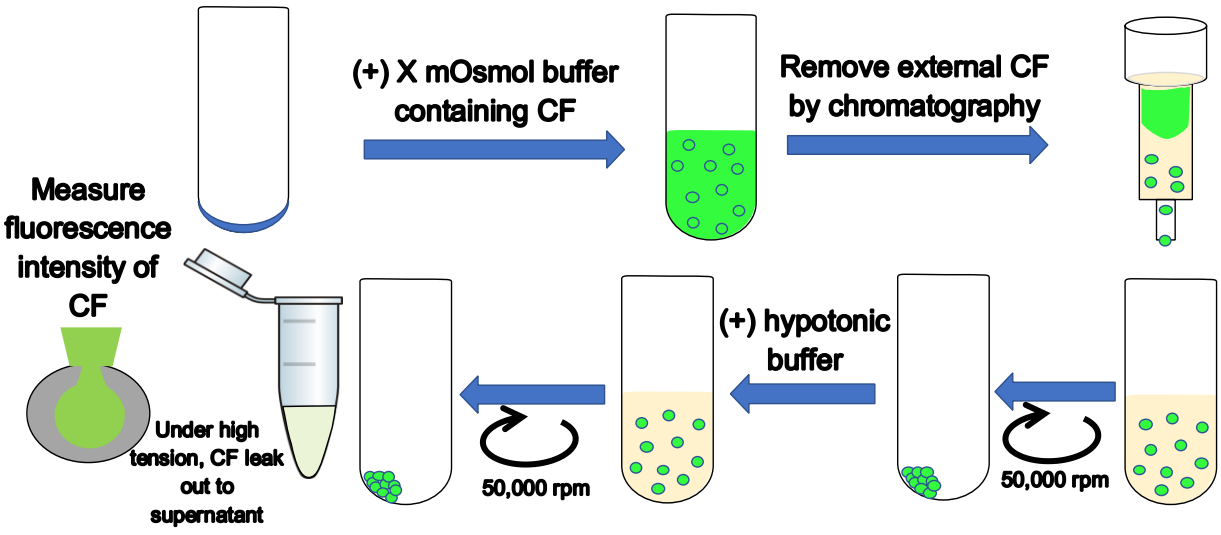

Figure 8: Osmotically-induced leakage assay to determine the limit tension for liposomes

First, I examined the CF release from the liposomes made of porcine brain Folch fraction, a total fraction of porcine brain, under several levels of hypotonic tension (Fig. 9A). The result showed that the leakage increased as the tension increases. Then I picked a tension induced by 160 mOsmol difference between inside and outside liposomes because this tension cause ~10% leakage.

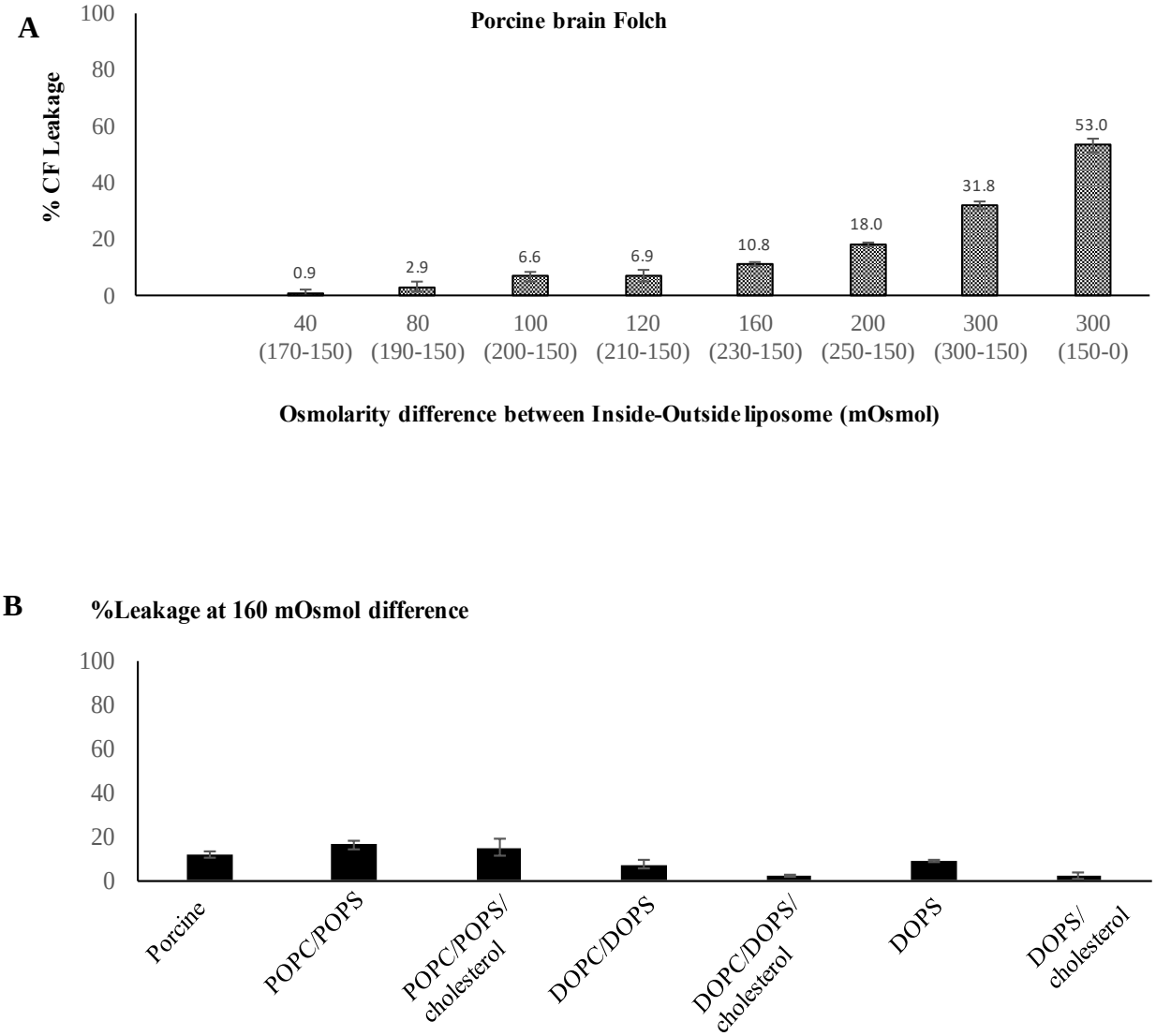

Figure 9: A. % carboxyfluorescein (CF) release from porcine brain Folch liposomes upon several level of tensions. B. % CF release from several types of liposomes at a tension induced by 160 mOsmol difference between inside and outside liposomes. Experiments were performed three times. Error bar indicates SD.

Then, I applied this tension to liposomes composed of various lipid compositions to confirm that this tension causes minimal leakage. As the results, the leakage percentage varies among the liposomes (Fig. 9B). The leakage was considered low (< 20%). Therefore, I selected 435 mOsmol sucrose as the solute inside liposomes, and 300 mOsmol outside, by using glucose buffer, under the same salt concentrations, and thus the osmolarity difference between inside and liposomes was 135 mOsmol.

3.2 Hypotonic tension stretched and loosen the lipid packing while cholesterol tighten the lipid packing

I attempted to confirm the existence of tension on the liposomal membrane. Even though the leakage occurred, the tension was thought to remain in the liposomes without rupture because the lipids in the liposome are experiencing stretching, indicating that this level of tension affects the physical properties of the liposomes.

To examine the tension applied to the membrane, I examined the lipid packing of the liposomes both under hypotonic tension and lack tension (isotonic) by using Laurdan fluorescence probe, which is embedded in the lipids and change the fluorescence by the packing, or more precisely on the environment of the surroundings. The Laurdan's emission shifts from blue to green in the ordered lipid phase of the membrane due to tight lipid packing, and shift from green to blue in the disordered or fluid lipid phase due to loose packing. Such shift in Laurdan's fluorescence can be expressed by the generalized polarization function (GP value), which are the ratio of the emission at the two wavelengths quantify the exposure of Laurdan to water, where GP value of 1 means no exposure of Laurdan to water, whereas GP value of -1 means the complete exposure of Laurdan to bulk water (Amaro et al., 2017; Golfetto et al., 2013; Sanchez et al., 2012).

I prepared liposomes composed of cholesterol, PC, and PS, which are abundant lipids in caveolae. PC and PS lipids are major phospholipids in caveolae (Ortegren et al., 2004; Razani et al., 2002; Smart et al., 1999; Zeghari et al., 2000,), and palmitic acid (16:0) and oleic acid (18:1) were reported to be abundant fatty acids in caveolae (Cai et al., 2013; Huot et al., 2010). In addition to phospholipids, cholesterol has been known to be essential in caveolae formation (Ortegren et al., 2004; Razani et al., 2002; Smart et al., 1999). Accordingly, I prepared the liposomes from 1-palmitoyl-2-oleoyl PC and PS lipids (POPC and POPS) (Fig. 10), in the presence and absence of

cholesterol. These liposomes exhibited ~16% rupture upon the hypoosmotic tension induced by the 300 mOsmol glucose (Fig. 9B).

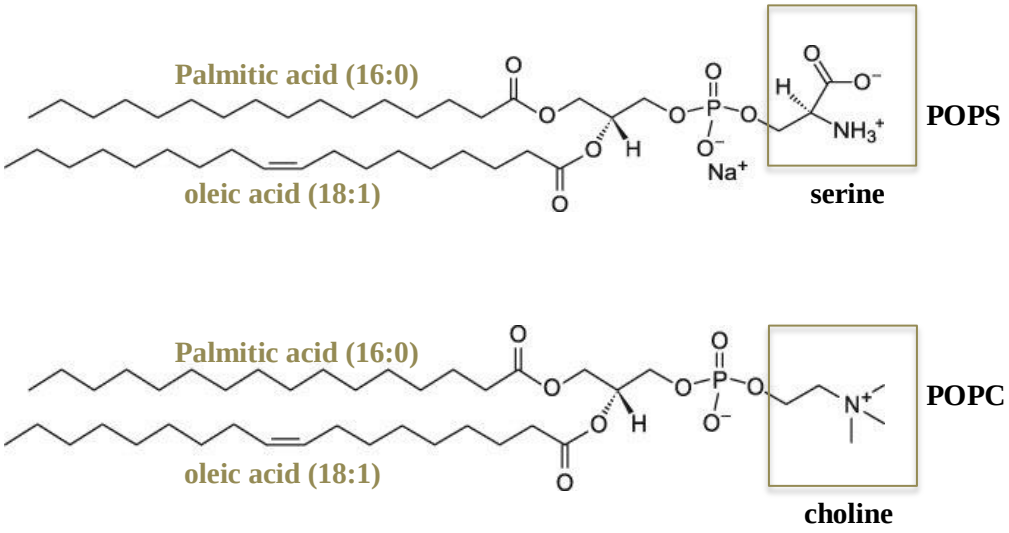

Figure 10: Lipid composition of liposomes. POPS and POPC contain major fatty acids in caveolae (palmitic acid (16:0) and oleic acid (18:1).

The laurdan fluorescence at 440 nm, which is blue emission, represents tight lipid packing, and that at 475 nm, which is green emission, indicates loose lipid packing (Fig. 11A). In POPC/POPS liposomes, in which cholesterol is absent, the emission intensity at 440 nm appeared to be similar to that at 475 nm in the presence or absence of tension. The presence of cholesterol in POPC/POPS/cholesterol shifted the emission peak to 440 nm, suggesting that cholesterol tighten the lipid packing. These results were then quantified by GP value. The GP value decreased when more water penetrates into the bilayer due to a loosening of lipid packing. GP value increases when less water penetrates into bilayer due to the tightening of lipid packing. The GP values (Fig. 11B) showed that tension lowered the GP value of POPC/POPS liposomes, indicating that tension stretches the lipids and loosen the packing. While tension did not significantly alter the GP value of POPC/POPS/cholesterol liposome, suggesting that tension was not sufficient to loosen the lipid packing of POPC/POPS/cholesterol liposomes, which contain a lot of packing defects for water penetration without tension (Fig. 11C). These data suggested that tension stretched the lipid packing only in the absence of cholesterol.

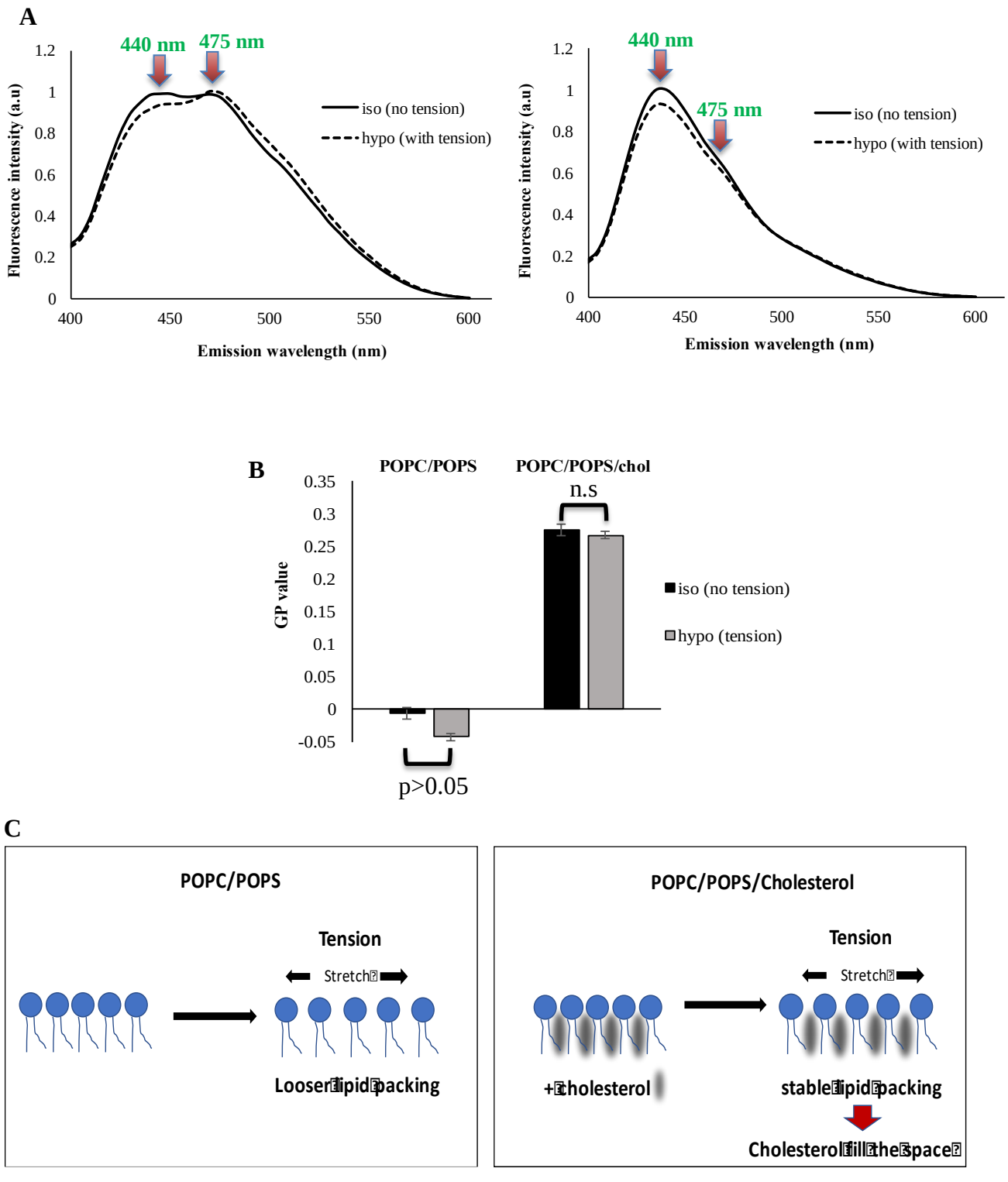

Figure 11: Laurdan fluorescence assay for lipid packing detection. A. Laurdan fluorescence intensity measurement (a.u) was performed under isotonic (no tension) and hypotonic tension. Lipids : Laurdan molar ratio is 1:1300. B. Generalized polarization (GP) chart. C. Lipid packing conditions in POPC/POPS and POPC/POPS/cholesterol. Tension loosen the lipid packing in the absence of cholesterol. The presence of cholesterol stabilizes the packing under tension. Experiments were performed 3 times, error bar indicates SD, paired-Ttest.

3.3 Hypotonic tension did not affect the binding affinity of PACSIN2 F-BAR to POPC/POPS and POPC/POPS/cholesterol liposomes

The removal of PACSIN2 from caveolae upon tension indicated that hypotonic tension removed PACSIN2 from caveolae. In cells, hypoosmotic tension induced the phosphorylation of PACSIN2 (Senju et al., 2015). However, it had been unclear whether the phosphorylated PACSIN2 had a weaker affinity to caveolar lipid membrane or tension directly weaken the PACSIN2 binding by opposing the deformation of the membrane by PACSIN2. Because the F-BAR domain is the membrane binding domain of PACSIN2, I then examined the binding affinity of PACSIN2 F-BAR to POPC/POPS and POPC/POPS/cholesterol liposomes, under both isotonic and hypotonic tension, by the liposome co-sedimentation assay (Fig. 12). Because the amount of the PACSIN2 proteins in the liposomal pellet (indicated by P) were similar independently of lipid composition and tension (Fig. 13), I found that the binding affinity of PACSIN2 F-BAR under both isotonic and hypotonic tension was similar, indicating that tension was independent of cholesterol. This result confirmed that hypotonic tension does not directly affect PACSIN2 F-BAR binding to the membrane, suggesting the removal of PACSIN2 from caveolae happened by the weaker affinity of the phosphorylated PACSIN2, as has been suggested from the binding to the brain Folch liposomes (Senju et al., 2015).

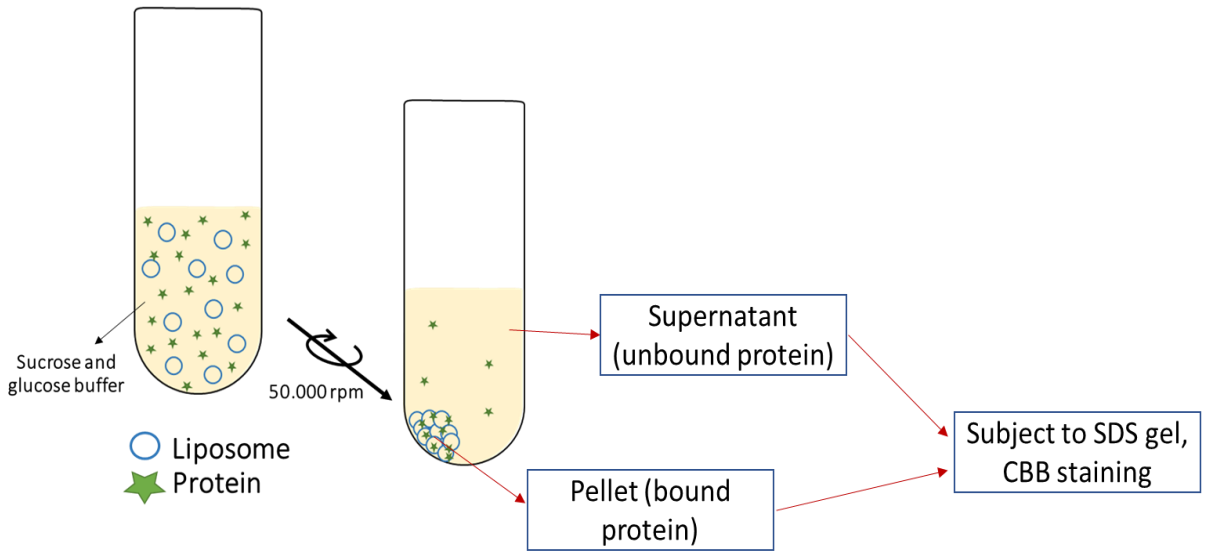

Figure 12: Liposome co-sedimentation assay

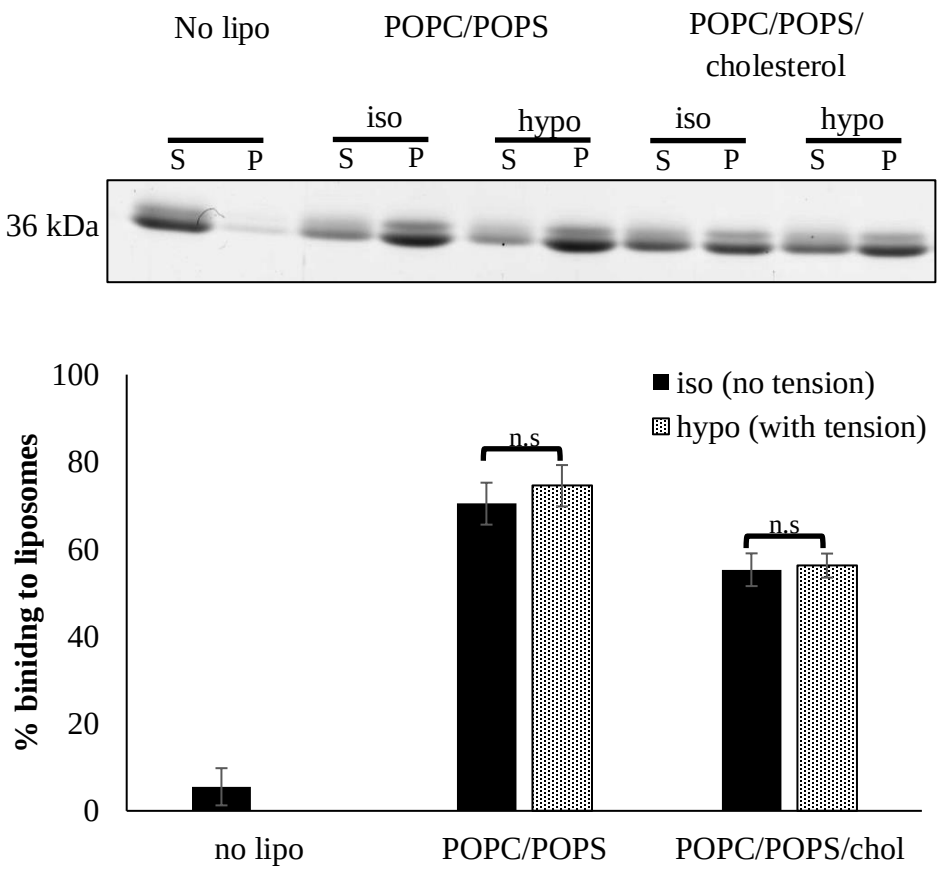

Figure 13: Binding affinity of PACSIN2 F-BAR (5 μM) to POPC/POPS and POPC/POPS/cholesterol under isotonic (no tension) and hypotonic tension by co-sedimentation assay. PACSIN2 F-BAR was incubated with liposomes, supernatant (S) was then separated from pellet (P) by ultracentrifuge. S and P were subjected to SDS gel and stained by CBB. Liposome concentration: 0.125 μg/μl. Assay was performed 4 times, error bar indicates SD, and statistically significance between iso and hypo condition was analyzed by paired T-test.

3.4 Cholesterol weaken the binding affinity of PACSIN2 to the liposomes

The effect of cholesterol on the binding affinity of PACSIN2 F-BAR was then investigated by determining the concentration of liposomes that is required for 50% binding (dissociation constant, Kd), by liposome co-sedimentation assay. The results are presented in Fig. 14, which shows the percentages of PACSIN2 F-BAR binding to liposomes in co-sedimentation assay dependent on the concentrations of liposomes (μg/μl). In POPC/POPS, the concentration of this liposome to reach 50% binding with PACSIN2 F-BAR was 0.10 μg/μl, while PACSIN2 F-BAR required more POPC/POPS/cholesterol, 0.24 μg/μl, to reach 50% binding.

One of the ways that PACSIN2 F-BAR interacts with cell membrane is through the interaction between positively-charged residues of F-BAR with negatively-charged phospholipids (Fig. 6). In this study, POPS was the negatively charged-phospholipids. In POPC/POPS, 0.10 µg/µl contained 53.1µM POPS, while in POPC/POPS/cholesterol, 0.24 µg/µl contained 84.9 µM POPS (Fig. 14A). The presence of cholesterol was thought to promote the formation of larger defect due to the formation of the ordered phase, which might result in ~40% decrease in the affinity by the presence of cholesterol. In this condition, PACSIN2 F-BAR required more POPS to reach 50% binding in the presence of cholesterol, or in other words, cholesterol weakened the binding of PACSIN2 F-BAR to the liposomes.

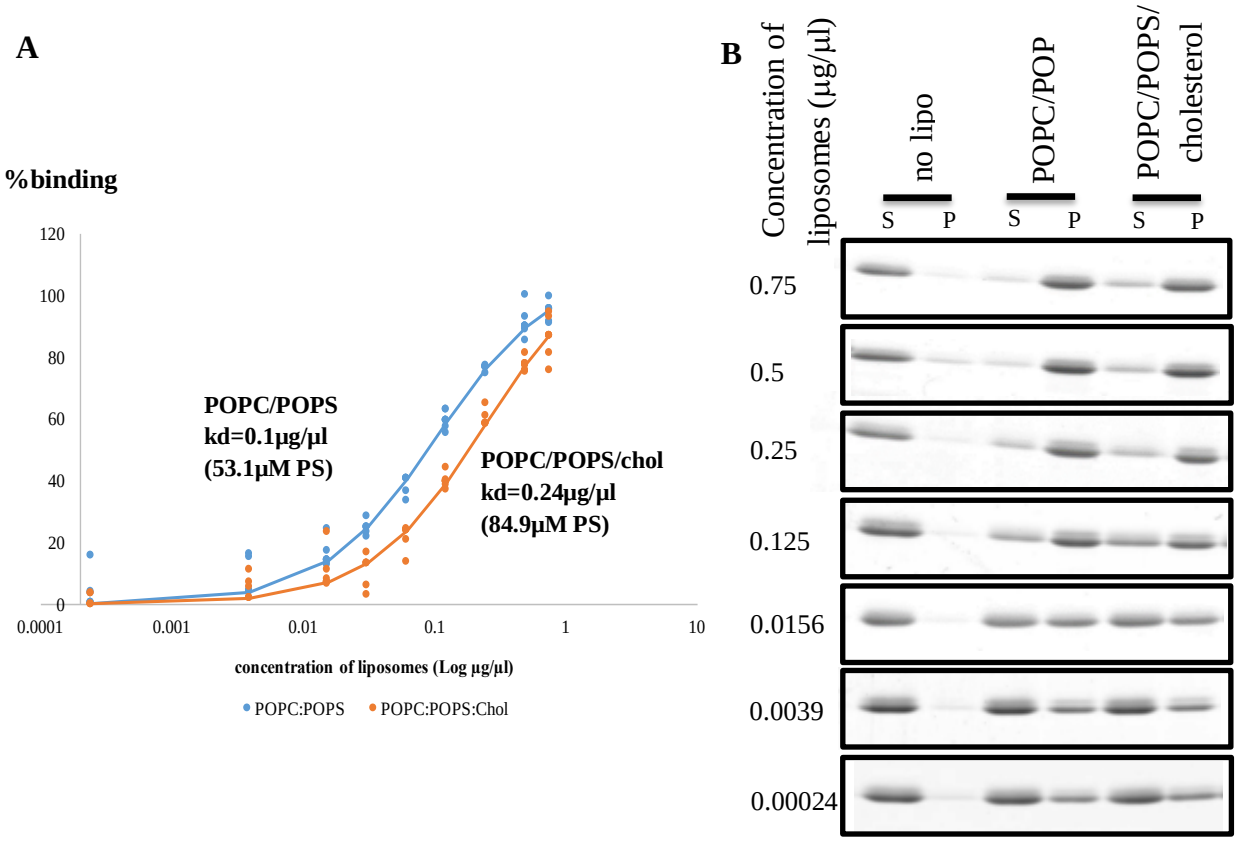

Figure 14: Dissociation constant (Kd) of purified PACSIN2 F-BAR (5µM) to liposomes made of POPC/POPS and POPC/POPS/cholesterol, determined by liposome co-sedimentation assay. PACSIN2 F-BAR was incubated with liposomes, supernatant (S) was then separated from pellet (P) by ultracentrifuge. S and P were subjected to SDS gel and stained by CBB. Kd graph represents % binding of PACSIN2 F-BAR against concentration of bound liposomes to PACSIN2 F-BAR. Experiments were performed at least 3 times each concentration of liposome. Kd value was analyzed by excel solver.

3.5 The phosphorylation mimetic PACSIN2 S313E mutant had reduced affinity to the cholesterol containing membrane

PACSIN2 phosphomimetic mutant (PACSIN2 S313E) was found to be decreased in liposome composed of bovine brain Folch (Senju et al., 2015). However, it remained unclear whether the decrease was cholesterol dependent because the decrease was observed with the liposomes made of bovine brain lipids, which contains cholesterol (Rouser et al., 1963; Vedaraman et al., 2004). Therefore, I performed liposome co-sedimentation assay to examine the binding affinity of PACSIN2 S313E and PACSIN2 to POPC/POPS and POPC/POPS/cholesterol. I found that the binding affinity of these two proteins to POPC/POPS liposomes was similar (Fig. 15). However, the binding of PACSIN2 to POPC/POPS/cholesterol liposomes was weaker than to POPC/POPS liposomes, consistent with binding of PACSIN2 F-BAR to liposomes and the previous report showing that PACSIN2 S313E had weaker affinity to the liposomes made of bovine brain Folch compared to PACSIN2 (Senju et al., 2015).

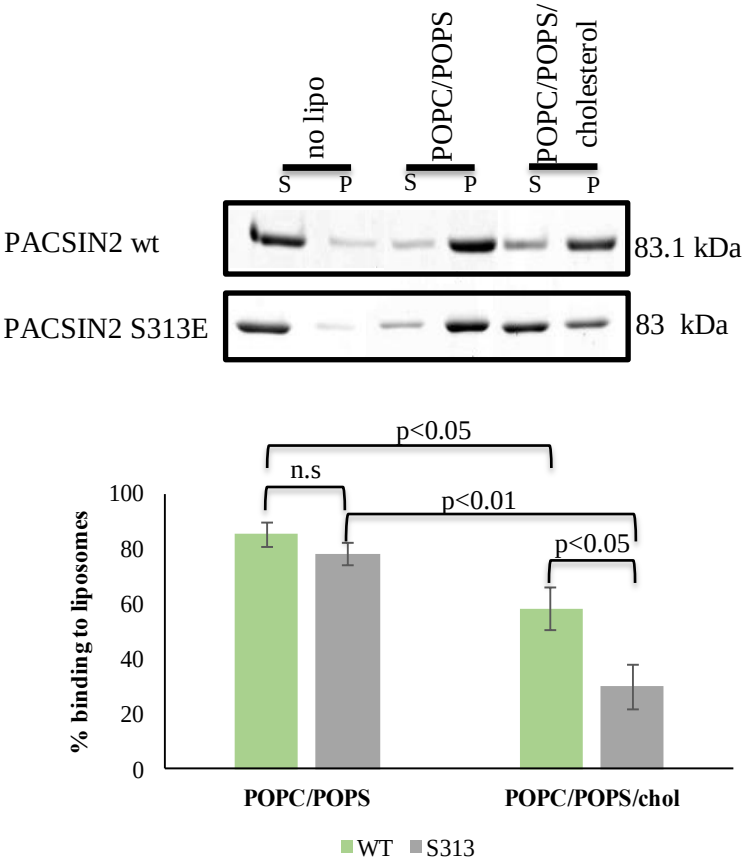

Figure 15: Binding affinity of PACSIN2 full length-mcherry and PACSIN2 S313E-mcherry to POPC/POPS and POPC/POPS/cholesterol liposomes by co-sedimentation assay. The assay was performed three times. Error bar indicates SD. Statistical significance data were analyzed using the Student's t-test.

3.6 Cholesterol, but not tension, altered the remodeling activity of PACSIN2

In order to investigate whether cholesterol influenced the membrane remodeling of PACSIN2, I next observed the morphology of liposomes in the presence of PACSIN2 F-BAR by transmission electron microscope (TEM). In POPC/POPS, PACSIN2 F-BAR deformed this liposome into tubular shapes. However, in POPC/POPS/cholesterol, no tubular shapes were observed. Instead, PACSIN2 remodeled this liposome into the formation of 'the beads on the string', with a size of ~100 nm (Fig. 16). The size of this beads-like shape might resemble the size and curvature of the flask-shaped caveolae. These results indicated that cholesterol suppressed the formation of straight tubules by PACSIN2 F-BAR and induced the formation of caveolae-like morphology in the liposome made of PO lipids.

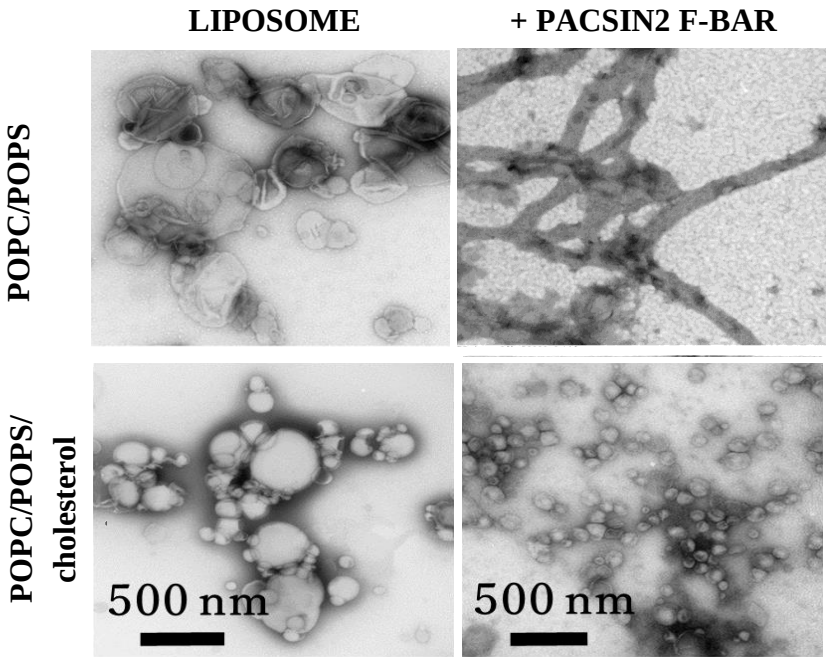

Figure 16: Negative-stain TEM. PACSIN2 F-BAR (5 μM) deform POPC/POPS liposome into tubular shape, and POPC/POPS/cholesterol into caveolae-associated morphology with size of ~100nm. Liposome concentration: 0.125 μg/μl.

The effect of hypotonic tension on PACSIN2 F-BAR remodeling activity was then observed by TEM. Under hypotonic tension, PACSIN2 F-BAR still deformed the POPC/POPS liposomes into tubular shape in a similar manner as under isotonic condition, and the formation of 'the beads on the string' in POPC/POPS/cholesterol remained unchanged (Fig. 17). These data suggested that hypotonic tension did not affect the binding and remodeling activity of PACSIN2 F-BAR.

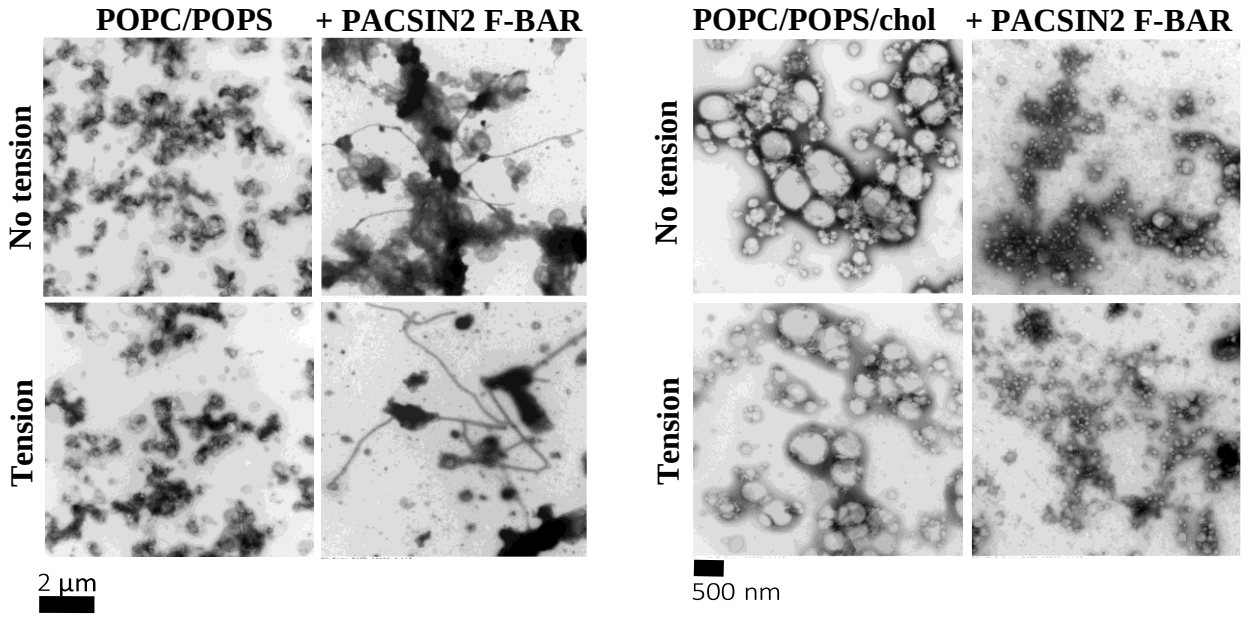

Figure 17: Negative stain TEM show the remodeling activity of PACSIN2 F-BAR (5 μM) to POPC/POPS and POPC/POPS/cholesterol under both isotonic and hypotonic tension. Liposome concentration: 0.125 μg/μl. Observations were independently performed three times.

3.7 Cholesterol and hypotonic tension did not alter the insertion depth of the hydrophobic loops of PACSIN2 F-BAR

I found that cholesterol reduced the binding affinity and remodeling activity of PACSIN2 F-BAR to the membrane. Since hypotonic tension stretched the lipid packing, I next examined whether cholesterol and hypotonic tension modulate the depth of PACSIN2 F-BAR loops insertion. To measure the depth of loop insertion, a tryptophan was inserted at the tip of the loop, to measure the distance from the bilayer center to the tip of the loop (Fig. 18A). In order to do this analysis, I constructed PACSIN2 F-BAR M124W mutant and prepared POPC/POPS and

POPC/POPS/cholesterol containing brominated phospholipids (Br_2-PC) (Fig. 18B). The quenching of tryptophan fluorescence by bromides was then measured by spectrofluorometer. As shown in Fig. 19, the tryptophan fluorescence tended to decrease as the amount of Br_2-PC increased. The quenching by 6,7 Br-PC was stronger than by 9,10 Br-PC, indicating that the position of the tip of the loop was closer to 6,7 position than to 9,10 in the acyl-chains of phospholipids. The distance of the 6,7 Br to the center of phospholipids bilayer was 11 Å, while the 9,10 Br was 8.3 Å away from the bilayer center (Fig. 18B) (Kyrychenko et al., 2017; Zhao and Kinnunen, 2002).

The depth of the loop from bilayer center was calculated by the parallax method (Chattopadhyay and London 1987) and revealed that in POPC/POPS the position of PACSIN2 F-BAR loop from bilayer center, under isotonic condition (no tension) and hypotonic tension were 10.3 ± 0.2 Å and 10.2 ± 0.5 Å, respectively (Fig. 19). While in POPC/POPS/cholesterol, the distances under isotonic and hypotonic conditions were 10.2 ± 0.6 Å and 9.7 ± 0.6 Å, respectively. There was no significant difference in the insertion depth between isotonic and hypotonic conditions. There was also no significant difference in the insertion depth between in the presence and in the absence of cholesterol, as well. However, the tryptophan fluorescence was more quenched in POPC/POPS than in POPC/POPS/cholesterol, presumably because the binding of PACSIN2 F-BAR to POPC/POPS was stronger than to POPC/POPS/cholesterol, as a result, there were more unbound PACSIN2 F-BAR in the solution. Weaker binding affinity causes a lesser number of the loops are inserted into liposomes, in consequence, lesser tryptophan were quenched by Br_2-PC. Taken together, these results suggested that tension and cholesterol did not alter the position PACSIN2 F-BAR hydrophobic loops insertion, even though cholesterol modified remodeling activity of PACSIN2 F-BAR and tension loosened the lipid packing in POPC/POPS liposomes, suggesting that the possible decrease of the charge density and the changes in other properties of the membrane in the presence of cholesterol reduced the affinity of PACSIN2 to the membrane.

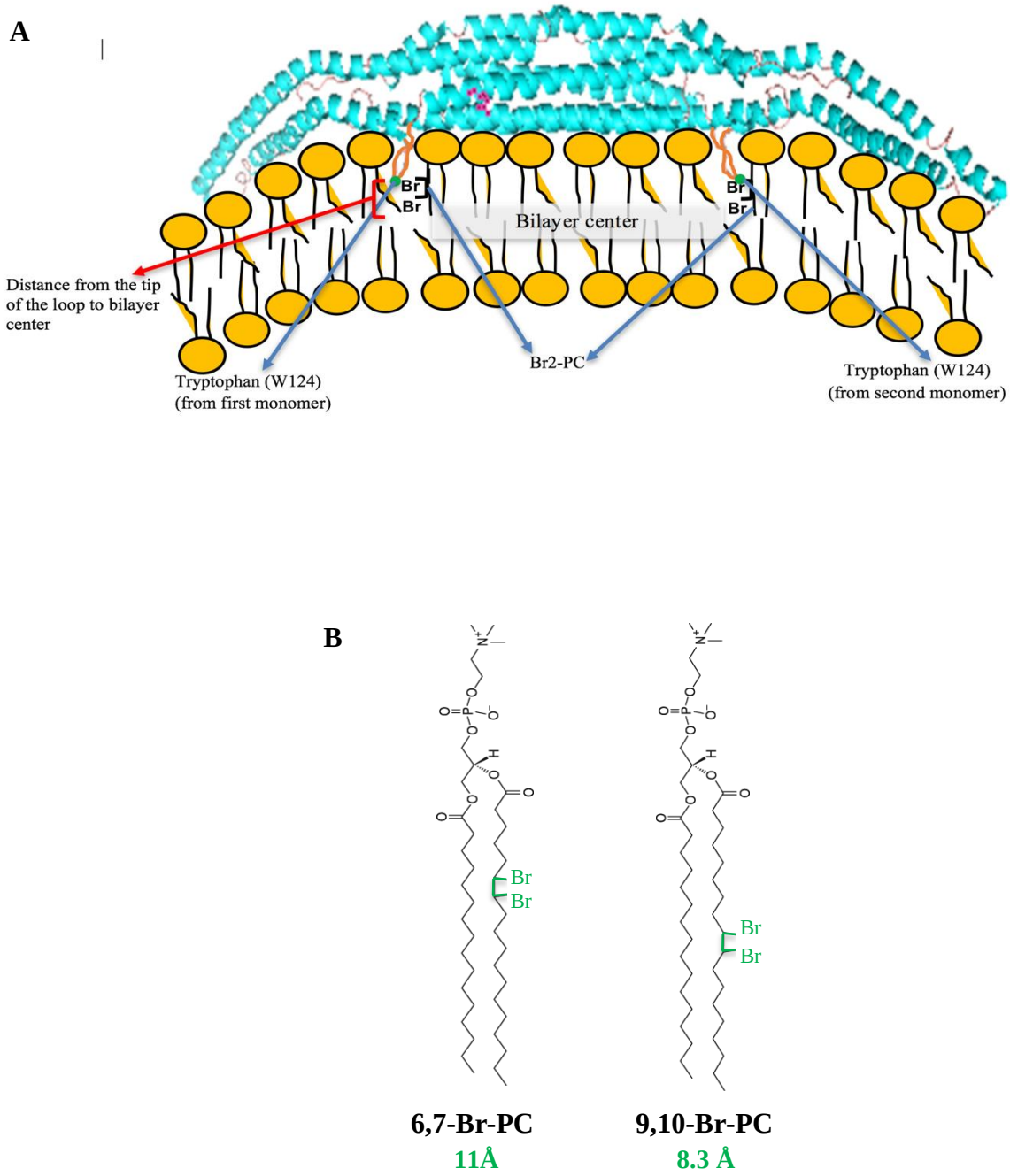

Figure 18: A. Illustration of PACSIN2 F-BAR hydrophobic loops insertion into liposomes containing brominated phosphatidylcholine (Br_2-PC). Bromides quench tryptophan fluorescence localized at the tip of the loop. Depth of insertion indicates the distance from the tip to the bilayer center. B. The structure of the quenchers used in this study and the distance from bilayer center to the quencher (Br).

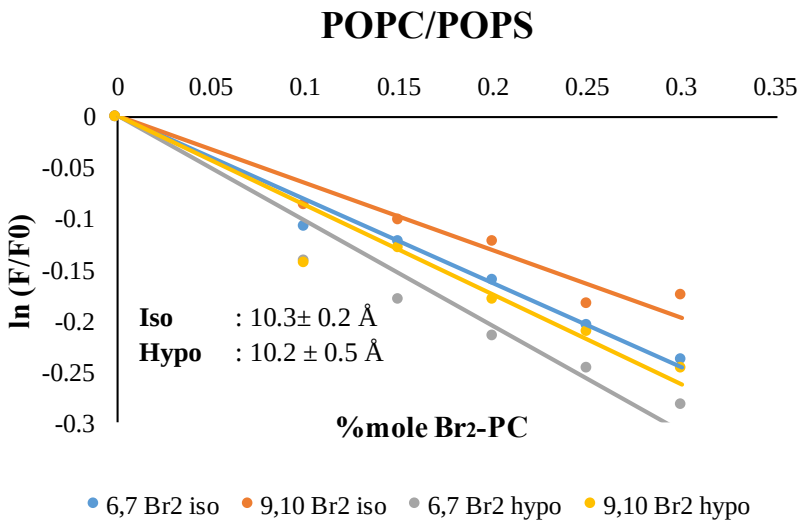

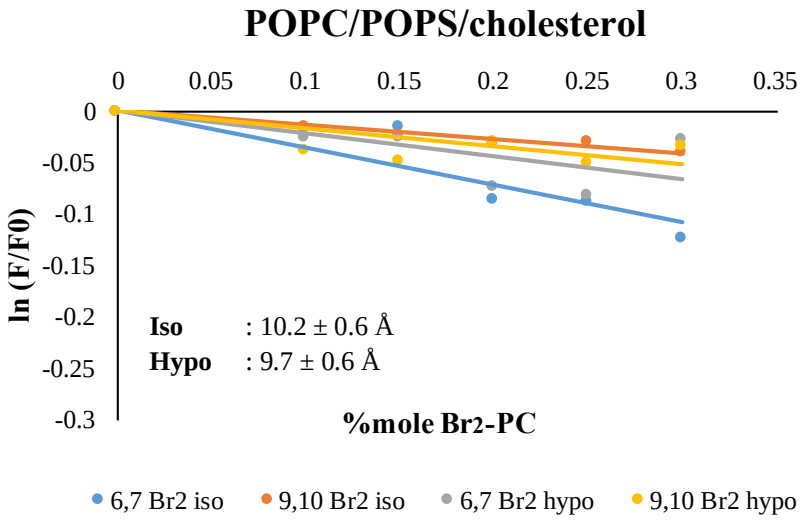

Figure 19: Fluorescence intensity (FI) of tryptophan in the presence of several %mol Br_2-PC (0.1; 0.15; 0.20; 0.25; 0.30), under both isotonic and hypotonic tension, presented as ln F/F0 with F = FI of tryptophan after quenching, F0= FI without quencher. PACSIN2 F-BAR: 5 µM, liposome concentration: 0.125 µg/µl.

3.8 The cholesterol dependency of the PACSIN2 binding depends on the specific acyl-chains of phospholipids

The di-palmitoyl and di-oleoyl lipids are also possible found in caveolae, although most phospholipids are supposed to be one saturated and one unsaturated acyl-chains (Pettitt 2009; Goto-Inoue et al. 2013; Pham et al. 2019; Skotland and Sandvig 2019; van Meer et al. 2008). I examined the binding affinity of PACSIN2 F-BAR on liposomes composed by DPPC/DPPS, di-palmitoyl (DP; 16:0-16:0) PC and PS, and DPPC/DPPS/cholesterol liposomes. DP lipids contain saturated fatty acid at both tails, and thus the liposomes made of these lipids have the tight lipid packing that inhibits the insertion of hydrophobic peptide (Bigay and Antonny, 2012) including PACSIN2 F-BAR loops (Fig. 20). The binding affinities of PACSIN2 F-BAR to both DPPC/DPPS and DPPC/DPPS/cholesterol liposomes were decreased compared with POPC/POPS and POPC/POPS/cholesterol liposomes as shown by the amount of the protein is the liposomal pellet (indicated by P in Fig. 21A). There was no difference in the affinities to DPPC/DPPS and DPPC/DPPS/cholesterol liposomes. The reduced binding to DP lipids compared to PO lipids indicated that the tight lipid packing of DP lipids inhibits the insertion of the loops. While similar binding of PACSIN2 to DPPC/DPPS liposomes and to DPPC/DPPS/cholesterol liposomes might indicate that DP membrane had phase separated in the presence of cholesterol (Choi et al. 2014; Miyoshi and Kato 2015), giving the same membrane in the presence or absence of cholesterols, and thus apparently being independent of cholesterol.

I also examined the binding affinity of PACSIN2 F-BAR to liposomes composed of DOPC/DOPS, in which both lipids have two oleic fatty acid chains (di-oleoyl (DO); 18:1-18:1), and DOPC/DOPS/cholesterol. The binding affinity of PACSIN2 F-BAR to these two types of liposomes was similar as shown in Fig. 21B. These results appeared to be correlated with the previous studies reporting that cholesterol has a strong tendency to escape from bilayers composed of DO lipids (Ali et al., 2007; Niu and Litman, 2002).

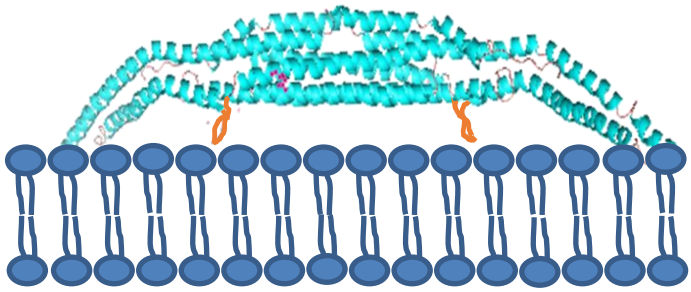

Figure 20: Tight lipid packing of DPPC/DPPS due to lack of unsaturated fatty acid prevents hydrophobic loop insertion, and thus the binding likely only happens through electrostatic interaction between F-BAR and DPPS.

3.9 PACSIN2 induced tubulation upon cholesterol depletion in cells

In order to investigate whether cholesterol could affect the PACSIN2-mediated membrane deformation in cells, the effect of cholesterol depletion on PACSIN2 F-BAR remodeling activity was investigated in HeLa cells expressing PACSIN2 F-BAR domain fragment. These cells were treated with Methyl-β-cyclodextrin (MβCD) to deplete cholesterol content from the plasma membrane. The cells under microscope were treated with MβCD, which gradually decreased the cholesterol on the plasma membrane. I found that cholesterol depletion induced acute tubulation of PACSIN2 F-BAR domain localization (Fig. 22). The similar tubulation of the full-length PACSIN2 was observed upon MβCD treatment, suggesting that cholesterol regulated the membrane deformation of full-length PACSIN2 (Fig. 22). These observations confirmed that cholesterol suppressed the formation of straight tubules of PACSIN2, or in other words, reduced remodeling activity of PACSIN2. This effect appeared to be correlated with the reduced binding affinity of PACSIN2 F-BAR in the presence of cholesterol in vitro (Fig. 14).

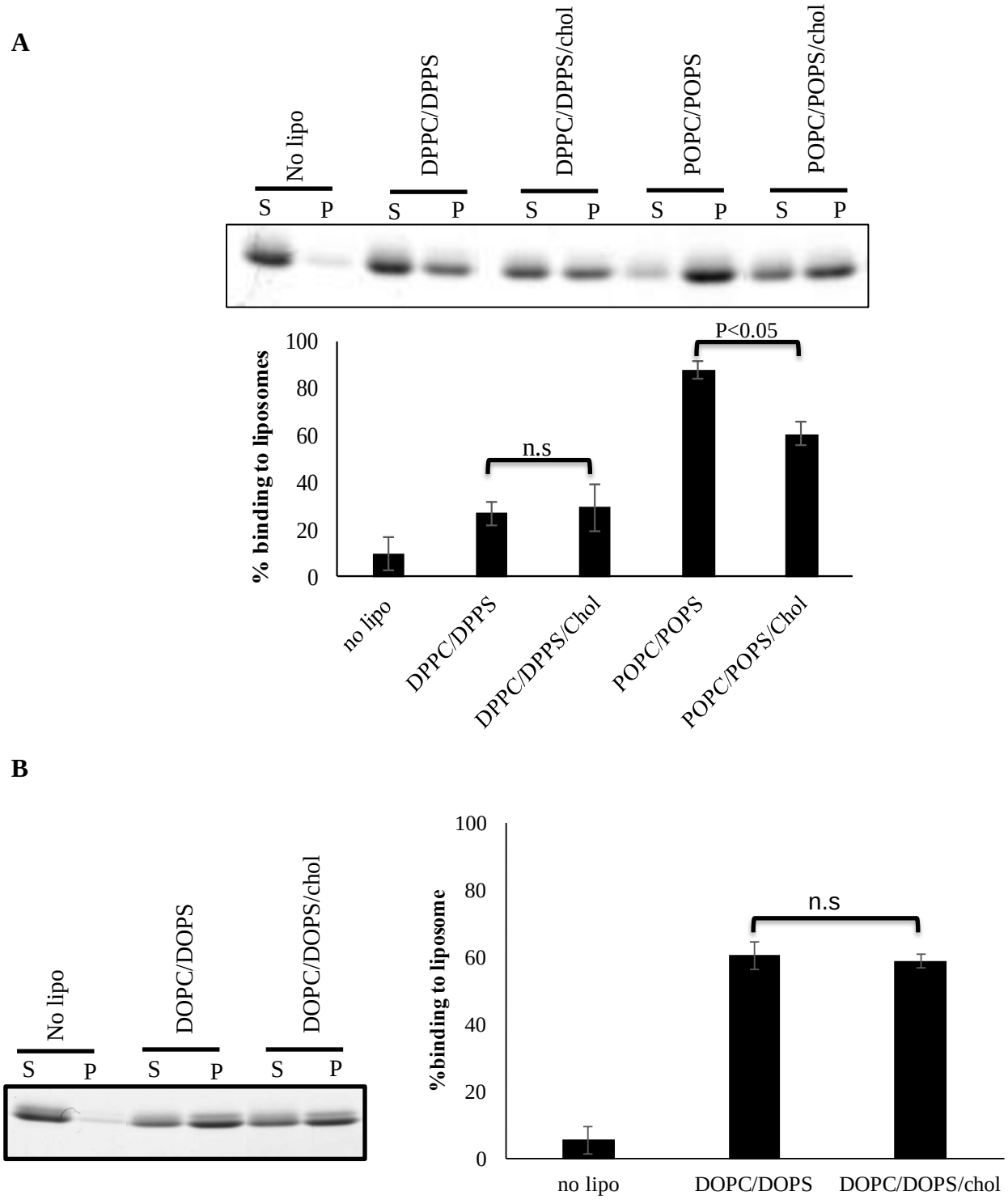

Figure 21: Binding affinity of PACSIN2 F-BAR (5μM) to A. DPPC/DPPS and DPPC/DPPS/cholesterol. B. DO (di-oleoyl; 18:1-18:1) PC/DOPS and DOPC/DOPS/cholesterol. Liposome concentration: 0.125μg/μl. Experiments were performed three times. Error bar indicates SD.

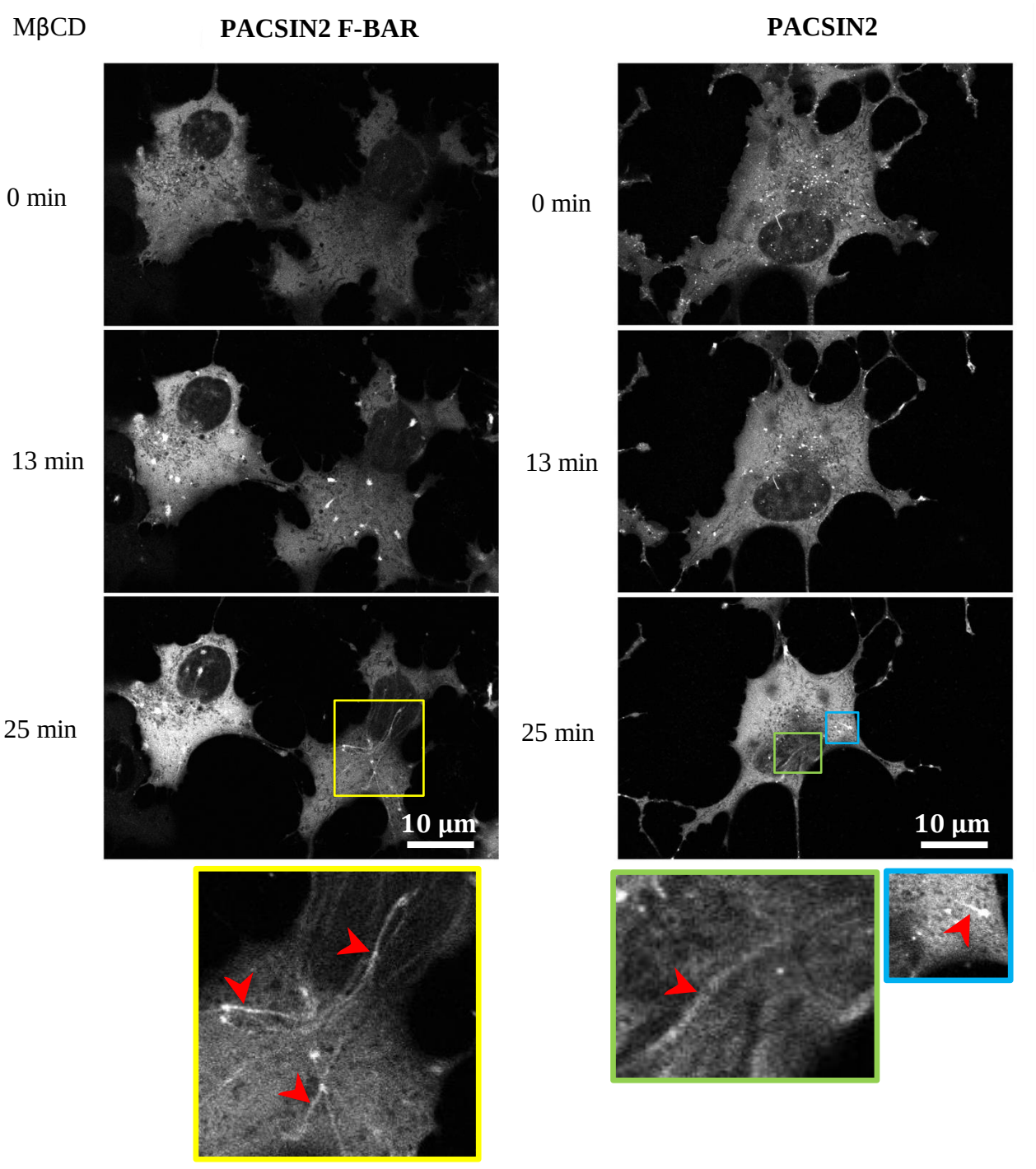

Figure 22: HeLa cells expressing PACSIN2 F-BAR and PACSIN2 full length show acute tubulations after methyl-β-cyclodextrin (MβCD) treatment. The tubulation started to appear at 13 min after cells were treated with MβCD.

3.10 PACSIN2 were transiently recruited to caveolae upon cholesterol depletion, presumably leading to the removal of caveolae

The effect of MβCD treatment on caveolae morphology was then observed. HeLa cells stably expressing PACSIN2-mCherry and caveolin-1 GFP at endogenous protein levels and then was treated with MβCD. PACSIN2 were transiently recruited to caveolin-1 and form acute tubulation with caveolin-1 localized at the tips (Fig. 23). Eventually, these tubules were disappeared simultaneously with the disappearance of caveolin-1 from plasma membrane. Therefore, these PACSIN2-localized tubules are considered to be the intermediates of endocytosis structures, because those tubules were shown to be increased by the inhibition of dynamin, a protein that executes membrane cutting in the endocytosis (Senju et al., 2011). This observation was consistent with previous studies that cholesterol depletion impairs caveolae morphology and lead to decrease the number of caveolae (Breen et al., 2012; Dreja et al., 2002; Parpal et al., 2001). These results also suggested that PACSIN2 remodel cholesterol-less membrane into tubular shape for presumable caveolae depletion through endocytosis and cholesterol-containing membrane into caveolae-associated morphology.

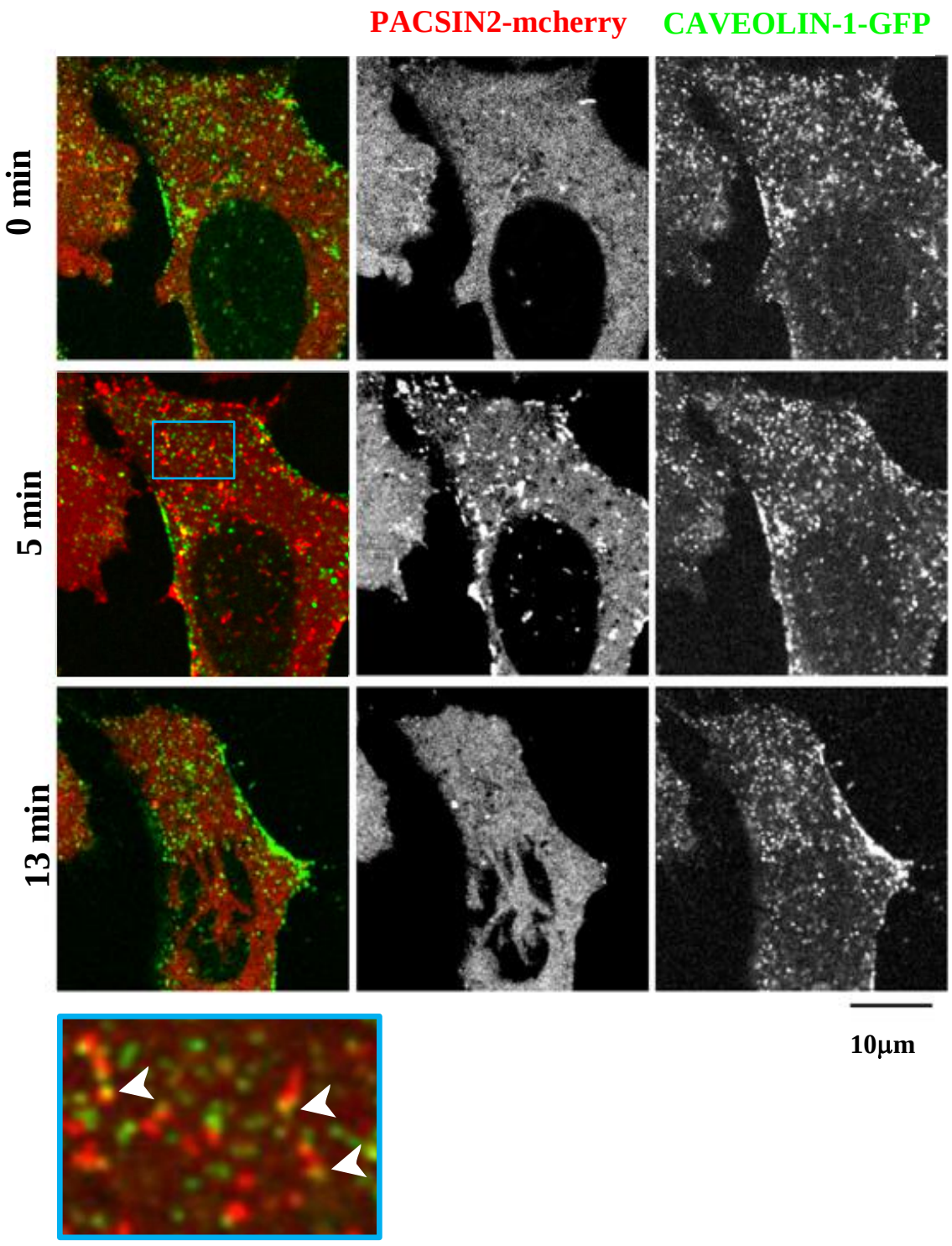

Figure 23: HeLa cells expressing PACSIN2-mcherry and caveoln-1-GFP after (MβCD) treatment show acute tubulation with caveolin-1 at the tip of the tubules. PACSIN2 were transiently recruited to the caveolin-1 associated membrane (shown in the blue box, pointed by white arrows) and impaired the morphology of caveolae followed by decrease of caveolae number.

4. DISCUSSION

In this study, I found that the membrane binding of PACSIN2 is negatively regulated by cholesterol in the membrane, using the reconstituted membrane containing the abundant lipids in caveolae, i.e., palmitoyl-oleoyl acid PC, PS, and cholesterol. Caveolae contain abundant cholesterol, presumably by the interaction with caveolin-1 (Fig.4). The localization of PACSIN2 at the neck of caveolar invaginations, not at the entire caveolar flask, appeared to be consistent with the negative regulation of membrane binding by cholesterol. The electron microscopic observations of the cholesterol-containing and cholesterol-less membranes in the presence of PACSIN2 indicated that the cholesterol can modulate the membrane shaping ability of PACSIN2, which is essential for caveolar morphogenesis, presumably for the shaping the caveolar neck. The previously suggested weakening of the membrane binding by the phosphorylation of PACSIN2 that happens upon the tension application to the cells were confirmed by using the cholesterol-containing membrane, while the tension itself did not significantly affect the membrane binding of PACSIN2. These in vitro data indicate that the lipid composition, rather than membrane tension, is the primary determinants for the membrane binding and membrane shaping by PACSIN2 (Fig. 13&14). Consistently, the depletion of cholesterol from the plasma membrane induced the PACSIN2 tubules that appeared to contain the elongated caveolae, which appeared to be the intermediate structure of caveolar endocytosis. Because cholesterol is known to be essential for caveolae structure, such tubular structure formation upon cholesterol decrease would be the mechanism for the downregulation of caveolae upon the decrease of cholesterol.

4.1 The membrane binding of PACSIN2 in the presence of cholesterol and under tension

The binding of PACSIN2 F-BAR to POPC/POPS and POPC/POPS/cholesterol were examined by the liposome co-sedimentation assay. The binding of PACSIN2 F-BAR to POPC/POPS/Cholesterol was weaker than that to POPC/POPS (Fig.14). Such difference in the binding appeared to be correlated with the presence of cholesterol in the membrane. Then, the presence of cholesterol is known to increase in the packing defects in the membrane. The charge density of the membrane decreases by the addition of cholesterol because of the slight increase in the membrane area. Therefore, the decreased affinity of PACSIN2 to the membrane by the

cholesterol might be explained by the decrease in the charge density by the cholesterol addition. Alternatively, the cholesterol makes some phase separated area on the membrane, and these areas of the membrane might not be capable of the PACSIN2 binding, thereby decreasing overall affinity of PACSIN2 to the membrane and the increase in the packing defects did not contribute to the binding of PACSIN2 to the membrane.

Next, the effect of tension on PACSIN2 F-BAR binding affinity to liposomes was investigated by applying hypotonic tension in a range of minimal membrane rupture (Fig.13). The application of the tension induced deeper packing defects on the membrane, which was confirmed by the laurdan fluorescence for the POPC/POPS membrane. The cholesterol addition also increased the packing defects, but the binding was not increased. Therefore, it might be from the packing defect would not be sufficient to promote the membrane binding of PACSIN2 to the membrane. In contrast, the tension-applied membrane with cholesterol did not have increase packing defects compared to the non-tension applied membrane. Therefore, no difference in the PACSIN2 binding to the membrane in the presence or absence of tension appears to be reasonable.

The morphology of liposomes was then examined by a transmission electron microscope (TEM). The POPC/POPS/Cholesterol liposomes were deformed by PACSIN2 F-BAR domain into 'the beads on the string' morphology, which might resemble the curvature of the flask-shaped caveolae. This beads on the string morphology was previously reported also by using the bovine brain Folch fraction, which contain cholesterol (Wang et al. 2009). In contrast, POPC/POPS liposomes without cholesterol were deformed by PACSIN2 F-BAR domain into straight tubules. Therefore, the change in the affinity of PACSIN2 to the membrane might induce the change in morphology of the membrane. It is also possible that cholesterol in the membrane changes the membrane deformability, thereby resulting in the different morphology of the liposomes in the presence of PACSIN2.

The effect of cholesterol in altering binding affinity and remodeling activity of PACSIN2 appeared to be similar in the plasma membrane of HeLa cells expressing PACSIN2 F-BAR and the full-length PACSIN2. Acute cholesterol depletion induced tubulation by PACSIN2 F-BAR and PACSIN2 in this cell. Such tubules contained caveolin-1, therefore suggesting that the removal of caveolae upon cholesterol depletion was involved in their endocytosis. Together, these data suggest that PACSIN2 deforms cholesterol-less membrane into tubular shape. However, in the presence of cholesterol, PACSIN2 deforms the membrane into caveolar morphology.

One of the possible mechanisms for the ability of cholesterol and tension to modulate PACSIN2 membrane binding was the modulation of the hydrophobic loop insertion. Surprisingly, the presence of cholesterol and tension did not change the depth of the loop insertion. Given that the presence of cholesterol reduced the binding of PACSIN2 F-BAR to the liposomes whereas the depth of the loop insertion remained unaltered, PACSIN2 F-BAR hydrophobic loops was suggested to be inserted in the space without cholesterol, and the presence of cholesterol in between the lipids might possibly inhibit the insertion. Because cholesterol increases the packing defects, such space might not be the same as the space that previously recognized as packing defect in space and time.

Some membrane proteins including caveolin-1 that have been reported to interact with cholesterol possess cholesterol binding motif that allows them to bind cholesterol. The presence of cholesterol in the membrane increases the binding of these proteins to this membrane (Fantini and Barrantes, 2013; Rosenhouse-Dantsker, 2017). Caveolin-1, for example, is known to have cholesterol recognition amino-acid consensus (CRAC) motif (Yang et al., 2014) and thus allow it to be recruited to cholesterol-rich membrane. This motif is not found in PACSIN2 F-BAR domain. Therefore, the reduced binding affinity of PACSIN2 in the presence of cholesterol might be resulted from the lack of cholesterol binding motif in PACSIN2.

In caveolae, PC, PS, and cholesterol are the major phospholipids. PC is well known to be the most abundant phospholipid that constitutes cell membrane, ranging from 41 to 57 mol % of the total glycerophospholipids (Yang et al., 2018; van Meer et al. 2008). PC is also one of phospholipids that are abundant in caveolae (Smart et al. 1999; Pike 2003; Huot et al. 2010). PS is a negatively charged phospholipid which is important for the binding of PACSIN2 F-BAR through the electrostatic interaction (Wang et al. 2009; Frost et al. 2009). Other important negatively-charged phospholipids in caveolae are phosphatidylinositol 4-phosphate (PI4P) and phosphatidylinositol 4,5-bisphosphate ($PI(4,5)P_2$). However, acute depletion of these lipids has minimal impact on caveolae assembly, while PS was found to be essential for proper caveolae formation and dynamics, and chronic reduction of PS resulted in a loss of caveolae (Hirama et al. 2017), which might suggest that phosphoinositides were not necessary for the reconstitution experiments with PACSIN2. In addition, there is no specific binding pocket for PI4P and $PI(4,5)P_2$ in PACSIN2 F-BAR domain, suggesting that the membrane binding of PACSIN2 did not appear to be specifically dependent on the particular negatively charged lipids like PI4P and PI(4,5)P2

(Dharmalingam et al. 2009). Phosphatidylethanolamine (PE) is also reported to be a major phospholipid in caveolae (Hirama et al., 2017). However, we did not use PE in the reconstituted membrane because PE did not contribute to the membrane binding of PACSIN2 F-BAR domain.

Fatty acids that mainly constitute caveolae are mono-unsaturated fatty acid, oleic acid (C18:1) and saturated fatty acids of palmitic acid (C16:0) and stearic acid (C18:0) (Cai et al., 2013; Huot et al., 2010). The percentage of these lipids were 32-41.7%, 24.1-38%, and 30%, respectively, indicating that the oleic acid was combined with either of palmitic acid and stearic acid in the phospholipids of the caveolae, because most of the phospholipids are known to have one saturated fatty acid and one unsaturated fatty acid (Pettitt 2009; Goto-Inoue et al. 2013; Pham et al. 2019; Skotland and Sandvig 2019; van Meer et al. 2008). Therefore, the lipids with palmitic acid (C16:0) and oleic acid (C18:1) (PO lipids) appeared to be suitable for the phospholipids of reconstituted membrane. We had not used the lipids with stearic acid because of the phospholipids of palmitic-oleic and stearic-oleic did not appear to have significant different properties in term of lipid packing for hydrophobic loop insertion (Pokorny et al. 2008).

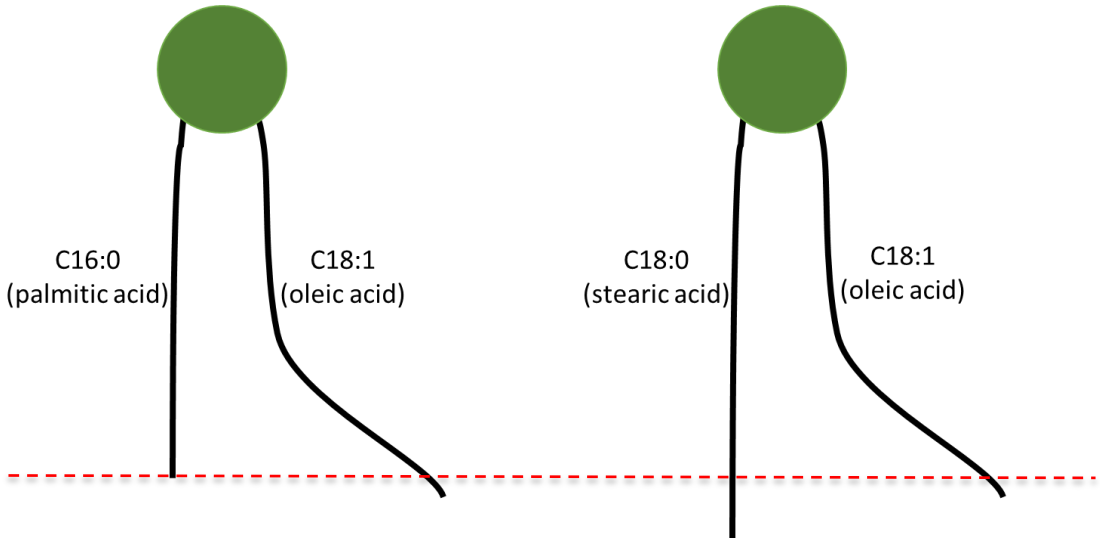

Figure 24: Illustration of phospholipids containing palmitic-oleic acids (16:0-18:1) and stearic-oleic acids (18:0-18:1). Stearic acid has longer carbon chain than palmitic acid.

To investigate the effect of the phosphorylation of PACSIN2 that occurs upon tension application to the cells in vitro, the phosphomimetic mutant of PACSIN2 (PACSIN2 S313E) was compared with full-length PACSIN2 for their membrane binding. The binding of PACSIN2 and PACSIN2 S313E to POPC/POPS remained similar. Interestingly, the binding of PACSIN2 S313E mutant to POPC/POPS/cholesterol was much weaker than that of PACSIN2. Therefore, the phosphorylation at Serine 313 weakens the PACSIN2 binding to cholesterol-containing membrane, which suggested the cholesterol is required for the removal of PACSIN2 from caveolae upon tension application indirectly through phosphorylation (Fig.7).

In contrast to the phospholipids with one mono-unsaturated and one saturated fatty acid, the lipids with both saturated and unsaturated fatty acids had different binding properties to PACSIN2. Phospholipids that contain oleic acid at both tails such as di-oleoyl (DO: 18:1-18:1) PC and PS (DOPC and DOPS) did not exhibit the decrease in the binding upon the incorporation of cholesterol (Fig. 21B). The absence of cholesterol dependency on PACSIN2 binding with di-oleoyl (DO) lipids may be consistent with the previous studies reporting that cholesterol has strong tendency to escape from bilayers composed of DO lipids (Ali et al., 2007; Niu and Litman, 2002). I also examined the binding affinity of PACSIN2 F-BAR to DPPC/DPPS, di-palmitoyl (DP; 16:0-16:0) PC and PS, and DPPC/DPPS/cholesterol. The binding affinity of PACSIN2 F-BAR to these liposomes was much lower than to PO lipids, and the presence of cholesterol had no significant effect on the binding (Fig. 21A). DP lipids are saturated fatty acids, therefore, induce the formation of tight lipid packing, which inhibits the insertion of the hydrophobic loops of PACSIN2 F-BAR (Fig. 20) as for the amphipathic helices that are inserted into the membrane (Bigay and Antonny, 2012).

4.2 The possible role of PACSIN2 for maintenance of cholesterol-rich caveolae

In this study, I found that the membrane binding of PACSIN2 is negatively regulated by cholesterol and independent of tension under membrane rupture. The neck of caveolae is the region where the cholesterol concentration at caveolae starts to decrease. Therefore, PACSIN2 localization at the neck of caveolae is thought to have resulted from the lower binding of PACSIN2 to the cholesterol-containing membrane than the plasma membrane with lesser amount of cholesterol. The analysis of PACSIN2 localization by using the cells with a decrease of plasma membrane cholesterol supported the negative regulation of the membrane binding of PACSIN2 for

caveolae maintenance. Therefore, PACSIN2 is suggested to remodel the membrane dependent on cholesterol for caveolar morphology. The decrease in the affinity of PACSIN2 in the membrane-bindings presumably due to the decreased charge density of the membrane by the presence of cholesterol, not by the alteration in the packing defects. In summary, this study has identified the differential behaviors of PACSIN2 in remodeling of cholesterol-less membrane and cholesterol containing-membrane. PACSIN2 deform POPC/POPS liposomes into tubules and POPC/POPS/cholesterol liposomes into the beads on the string formation, which resemble caveolae associated morphology. These differential activities are independent of tension. In cell, PACSIN2 remodel cholesterol-less membrane into tubular shape. In contrast, without cholesterol, PACSIN2 has been shown to be localized to the neck of caveolae (Senju et al. 2011; Hansen et al. 2011; Koch et al. 2012; Suetsugu and Gautreau 2012) (Fig. 25). Therefore, PACSIN2 is strongly suggested to remodel caveolae membrane tubules dependently on the cholesterol content.

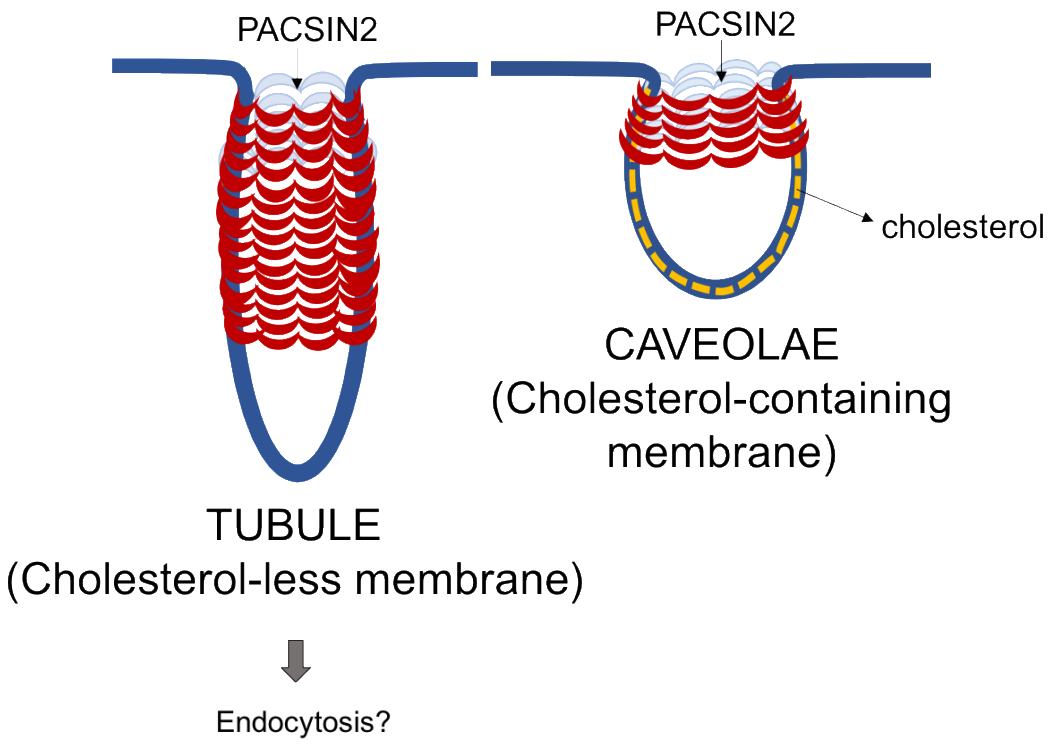

Figure 25: PACSIN2 remodeling activity in cholesterol-less membrane and cholesterol-containing membrane

5. ACKNOWLEDGEMENTS

Firstly, I would like to express my sincere gratitude to my supervisor Prof. Dr. Shiro Suetsugu for giving me the opportunity to join in his lab, for the continuous support and guidance of my PhD study, for his patience, and motivation. His great knowledge helped me in all the time of research and writing of this thesis. I would also like to thank to my second supervisor, Dr. Kyoko Hanawa-Suetsugu, for all her support. She has always been open to discussion. She also warms up the lab with offers for snacks and drink. I would like to thank to our laboratory Assistant Professors, Dr. Tamako Nishimura and Dr. Takehiko Inaba for all their supports especially during my adviser hearing preparation.

My sincere gratitude to my thesis committee: Prof. Dr. Naoyuki Inagaki and Dr. Noriaki Sasai, for their insightful comments and encouragement, but also for the hard questions which incented me to widen my research from various perspectives.

My sincere thanks also goes to Dr. Kazuma Yasuhara, who taught many things about liposomes, who gave access to his laboratory and research facilities and guided me during my work in his laboratory. Without his precious support it would not be possible to conduct this research.

I am grateful to the Japanese Government who supported my study through MEXT scholarship. Special thanks to NAIST staff and committee for the assistance and providing the funding for the work, especially Dr. Satoko Maki for her unfailing support and assistance.

Thanks also go to laboratory staff and my fellow labmates, from 2015 to now, for their continuous support. My fellow labmates who have made working in the lab an enjoyable experience, Sarah, Nhung, Izzati, Ting, Pei Fang, and Pang.

Finally, my time in NAIST would not have been so delightful without my friends especially from Indonesian community. Special thanks to Ria, mba Septi, mba Dewi, Emi, Rara, Maharani and Gema who have helped me through hard times. And last, but not least, a huge thank you to my family, Apa, Ama, Uni Rahma, and Rani, for always being there when I needed someone to talk to, for their love and continuous support.

6. REFERENCES

Alam Shibly, S.U., Ghatak, C., Sayem Karal, M.A., Moniruzzaman, M. and Yamazaki, M. 2016. Experimental estimation of membrane tension induced by osmotic pressure. *Biophysical Journal* 111(10), pp. 2190–2201.

Ali, M.R., Cheng, K.H. and Huang, J. 2007. Assess the nature of cholesterol-lipid interactions through the chemical potential of cholesterol in phosphatidylcholine bilayers. *Proceedings of the National Academy of Sciences of the United States of America* 104(13), pp. 5372–5377.

Amaro, M., Reina, F., Hof, M., Eggeling, C. and Sezgin, E. 2017. Laurdan and Di-4-ANEPPDHQ probe different properties of the membrane. *Journal of physics D: Applied physics* 50(13), p. 134004.

Bai, X.-L., Yang, X.-Y., Li, J.-Y., et al. 2017. Cavin-1 regulates caveolae-mediated LDL transcytosis: crosstalk in an AMPK/eNOS/ NF-κB/Sp1 loop. *Oncotarget* 8(61), pp. 103985–103995.

Bigay, J. and Antonny, B. 2012. Curvature, lipid packing, and electrostatics of membrane organelles: defining cellular territories in determining specificity. *Developmental Cell* 23(5), pp. 886–895.

Breen, M.R., Camps, M., Carvalho-Simoes, F., Zorzano, A. and Pilch, P.F. 2012. Cholesterol depletion in adipocytes causes caveolae collapse concomitant with proteosomal degradation of cavin-2 in a switch-like fashion. *Plos One* 7(4), p. e34516.

Buccione, R., Orth, J.D. and McNiven, M.A. 2004. Foot and mouth: podosomes, invadopodia and circular dorsal ruffles. *Nature Reviews. Molecular Cell Biology* 5(8), pp. 647–657.

Cai, Q., Guo, L., Gao, H. and Li, X.-A. 2013. Caveolar fatty acids and acylation of caveolin-1. *Plos One* 8(4), p. e60884.

Carlton, J., Bujny, M., Peter, B.J., et al. 2004. Sorting nexin-1 mediates tubular endosome-to-TGN transport through coincidence sensing of high- curvature membranes and 3-phosphoinositides. *Current Biology* 14(20), pp. 1791–1800.

Chattopadhyay, A. and London, E. 1987. Parallax method for direct measurement of membrane penetration depth utilizing fluorescence quenching by spin-labeled phospholipids. Biochemistry 26(1), pp. 39–45.

Choi, Y., Attwood, S.J., Hoopes, M.I., Drolle, E., Karttunen, M. and Leonenko, Z. 2014. Melatonin directly interacts with cholesterol and alleviates cholesterol effects in dipalmitoylphosphatidylcholine monolayers. Soft matter 10(1), pp. 206–213.

Chou, C.Y., Shen, M.R., Hsu, K.S., Huang, H.Y. and Lin, H.C. 1998. Involvement of PKC-alpha in regulatory volume decrease responses and activation of volume-sensitive chloride channels in human cervical cancer HT-3 cells. *The Journal of Physiology* 512 (Pt 2), pp. 435–448.

Cui, H., Lyman, E. and Voth, G.A. 2011. Mechanism of membrane curvature sensing by amphipathic helix containing proteins. *Biophysical Journal* 100(5), pp. 1271–1279.

Dharmalingam, E., Haeckel, A., Pinyol, R., et al. 2009. F-BAR proteins of the syndapin family shape the plasma membrane and are crucial for neuromorphogenesis. The Journal of Neuroscience 29(42), pp. 13315–13327.

Davenport, K.R., Sohaskey, M., Kamada, Y., Levin, D.E. and Gustin, M.C. 1995. A second osmosensing signal transduction pathway in yeast. Hypotonic shock activates the PKC1 protein kinase-regulated cell integrity pathway. *The Journal of Biological Chemistry* 270(50), pp. 30157–30161.

Dewulf, M., Köster, D.V., Sinha, B., et al. 2019. Dystrophy-associated caveolin-3 mutations reveal that caveolae couple IL6/STAT3 signaling with mechanosensing in human muscle cells. *Nature Communications* 10(1), p. 1974.

Dreja, K., Voldstedlund, M., Vinten, J., Tranum-Jensen, J., Hellstrand, P. and Swärd, K. 2002. Cholesterol depletion disrupts caveolae and differentially impairs agonist-induced arterial contraction. *Arteriosclerosis, Thrombosis, and Vascular Biology* 22(8), pp. 1267–1272.

Fairn, G.D., Schieber, N.L., Ariotti, N., et al. 2011. High-resolution mapping reveals topologically distinct cellular pools of phosphatidylserine. *The Journal of Cell Biology* 194(2), pp. 257–275.

Fantini, J. and Barrantes, F.J. 2013. How cholesterol interacts with membrane proteins: an exploration of cholesterol-binding sites including CRAC, CARC, and tilted domains. *Frontiers in physiology* 4, p. 31.

Finkelstein, A., Zimmerberg, J. and Cohen, F.S. 1986. Osmotic swelling of vesicles: its role in the fusion of vesicles with planar phospholipid bilayer membranes and its possible role in exocytosis. *Annual Review of Physiology* 48, pp. 163–174.

Frank, P.G., Pavlides, S. and Lisanti, M.P. 2009. Caveolae and transcytosis in endothelial cells: role in atherosclerosis. *Cell and Tissue Research* 335(1), pp. 41–47.

Frank, P.G., Woodman, S.E., Park, D.S. and Lisanti, M.P. 2003. Caveolin, caveolae, and endothelial cell function. *Arteriosclerosis, Thrombosis, and Vascular Biology* 23(7), pp. 1161–1168.

Frost, A., Perera, R., Roux, A., et al. 2008. Structural basis of membrane invagination by F-BAR domains. *Cell* 132(5), pp. 807–817.

Frost, A., Unger, V.M. and De Camilli, P. 2009. The BAR domain superfamily: membrane-molding macromolecules. *Cell* 137(2), pp. 191–196.

Gallop, J.L., Jao, C.C., Kent, H.M., et al. 2006. Mechanism of endophilin N-BAR domain-mediated membrane curvature. *The EMBO Journal* 25(12), pp. 2898–2910.

Golfetto, O., Hinde, E. and Gratton, E. 2013. Laurdan fluorescence lifetime discriminates cholesterol content from changes in fluidity in living cell membranes. *Biophysical Journal* 104(6), pp. 1238–1247.

Goto-Inoue, N., Yamada, K., Inagaki, A., et al. 2013. Lipidomics analysis revealed the phospholipid compositional changes in muscle by chronic exercise and high-fat diet. *Scientific reports* 3, p. 3267.

Hamai, C., Cremer, P.S. and Musser, S.M. 2007. Single giant vesicle rupture events reveal multiple mechanisms of glass-supported bilayer formation. *Biophysical Journal* 92(6), pp. 1988–1999.

Hansen, C.G., Howard, G. and Nichols, B.J. 2011. Pacsin 2 is recruited to caveolae and functions in caveolar biogenesis. *Journal of Cell Science* 124(Pt 16), pp. 2777–2785.

Heberle, F.A., Wu, J., Goh, S.L., Petruzielo, R.S. and Feigenson, G.W. 2010. Comparison of three ternary lipid bilayer mixtures: FRET and ESR reveal nanodomains. *Biophysical Journal* 99(10), pp. 3309–3318.

Hermoso, M., Olivero, P., Torres, R., Riveros, A., Quest, A.F.G. and Stutzin, A. 2004. Cell volume regulation in response to hypotonicity is impaired in HeLa cells expressing a protein kinase Calpha mutant lacking kinase activity. *The Journal of Biological Chemistry* 279(17), pp. 17681–17689.

Hirama, T., Das, R., Yang, Y., et al. 2017. Phosphatidylserine dictates the assembly and dynamics of caveolae in the plasma membrane. *The Journal of Biological Chemistry* 292(34), pp. 14292–14307.

Huot, P.S.P., Sarkar, B. and Ma, D.W.L. 2010. Conjugated linoleic acid alters caveolae phospholipid fatty acid composition and decreases caveolin-1 expression in MCF-7 breast cancer cells. *Nutrition research (New York, N.Y.)* 30(3), pp. 179–185.

Hutchison, J.B., Karunanayake Mudiyanselage, A.P.K.K., Weis, R.M. and Dinsmore, A.D. 2016. Osmotically-induced tension and the binding of N-BAR protein to lipid vesicles. *Soft matter* 12(8), pp. 2465–2472.

Jarsch, I.K., Daste, F. and Gallop, J.L. 2016. Membrane curvature in cell biology: An integration of molecular mechanisms. *The Journal of Cell Biology* 214(4), pp. 375–387.

Jung, W., Sierecki, E., Bastiani, M., et al. 2018. Cell-free formation and interactome analysis of caveolae. *The Journal of Cell Biology* 217(6), pp. 2141–2165.

Kessels, M.M. and Qualmann, B. 2004. The syndapin protein family: linking membrane trafficking with the cytoskeleton. *Journal of Cell Science* 117(Pt 15), pp. 3077–3086.

Kitamura, T., Koshino, Y., Shibata, F., Oki, T., Nakajima, H., Nosaka, T., and Kumagai, H. (2003). Retrovirus-mediated gene transfer and expression cloning: powerful tools in functional genomics. Experimental hematology 31, 1007-1014.

Knævelsrud, H., Søreng, K., Raiborg, C., et al. 2013. Membrane remodeling by the PX-BAR protein SNX18 promotes autophagosome formation. *The Journal of Cell Biology* 202(2), pp. 331–349.

Koch, D., Westermann, M., Kessels, M.M. and Qualmann, B. 2012. Ultrastructural freeze-fracture immunolabeling identifies plasma membrane-localized syndapin II as a crucial factor in shaping caveolae. *Histochemistry and Cell Biology* 138(2), pp. 215–230.

Kovtun, O., Tillu, V.A., Ariotti, N., Parton, R.G. and Collins, B.M. 2015. Cavin family proteins and the assembly of caveolae. *Journal of Cell Science* 128(7), pp. 1269–1278.

Kyrychenko, A., Posokhov, Y.O., Vargas-Uribe, M., Ghatak, C., Rodnin, M.V. and Ladokhin, A.S. 2017. Fluorescence applications for structural and thermodynamic studies of membrane protein insertion. In: Geddes, C. D. ed. *Reviews in fluorescence 2016*. Reviews in Fluorescence. Cham: Springer International Publishing, pp. 243–274.

Le Lay, S. and Kurzchalia, T.V. 2005. Getting rid of caveolins: phenotypes of caveolin-deficient animals. *Biochimica et Biophysica Acta* 1746(3), pp. 322–333.

Liu, X., Zhang, M.I.N., Peterson, L.B. and O'Neil, R.G. 2003. Osmomechanical stress selectively regulates translocation of protein kinase C isoforms. *FEBS Letters* 538(1–3), pp. 101–106.

Masuda, M., Takeda, S., Sone, M., et al. 2006. Endophilin BAR domain drives membrane curvature by two newly identified structure-based mechanisms. *The EMBO Journal* 25(12), pp. 2889–2897.

Miyoshi, T. and Kato, S. 2015. Detailed Analysis of the Surface Area and Elasticity in the Saturated 1,2-Diacylphosphatidylcholine/Cholesterol Binary Monolayer System. Langmuir: the ACS Journal of Surfaces and Colloids 31(33), pp. 9086–9096.

McMahon, H.T. and Boucrot, E. 2015. Membrane curvature at a glance. *Journal of Cell Science* 128(6), pp. 1065–1070.

van Meer, G., Voelker, D.R. and Feigenson, G.W. 2008. Membrane lipids: where they are and how they behave. *Nature Reviews. Molecular Cell Biology* 9(2), pp. 112–124.

Mim, C. and Unger, V.M. 2012. Membrane curvature and its generation by BAR proteins. *Trends in Biochemical Sciences* 37(12), pp. 526–533.

Modregger, J., Ritter, B., Witter, B., Paulsson, M. and Plomann, M. 2000. All three PACSIN isoforms bind to endocytic proteins and inhibit endocytosis. *Journal of Cell Science* 113 Pt 24, pp. 4511–4521.

Murata, M., Peränen, J., Schreiner, R., Wieland, F., Kurzchalia, T.V. and Simons, K. 1995. VIP21/caveolin is a cholesterol-binding protein. Proceedings of the National Academy of Sciences of the United States of America 92(22), pp. 10339–10343.

Niu, S.-L. and Litman, B.J. 2002. Determination of membrane cholesterol partition coefficient using a lipid vesicle-cyclodextrin binary system: effect of phospholipid acyl chain unsaturation and headgroup composition. *Biophysical Journal* 83(6), pp. 3408–3415.

Ortegren, U., Karlsson, M., Blazic, N., et al. 2004. Lipids and glycosphingolipids in caveolae and surrounding plasma membrane of primary rat adipocytes. *European Journal of Biochemistry / FEBS* 271(10), pp. 2028–2036.

Park, D.S., Woodman, S.E., Schubert, W., et al. 2002. Caveolin-1/3 double-knockout mice are viable, but lack both muscle and non-muscle caveolae, and develop a severe cardiomyopathic phenotype. *The American Journal of Pathology* 160(6), pp. 2207–2217.

Parpal, S., Karlsson, M., Thorn, H. and Strålfors, P. 2001. Cholesterol depletion disrupts caveolae and insulin receptor signaling for metabolic control via insulin receptor substrate-1, but not for mitogen-activated protein kinase control. *The Journal of Biological Chemistry* 276(13), pp. 9670–9678.

Parton, R.G. 2018. Caveolae: structure, function, and relationship to disease. *Annual Review of Cell and Developmental Biology* 34, pp. 111–136.

Patel, H.H. and Insel, P.A. 2009. Lipid rafts and caveolae and their role in compartmentation of redox signaling. *Antioxidants & Redox Signaling* 11(6), pp. 1357–1372.

Pathak, P. and London, E. 2015. The effect of membrane lipid composition on the formation of lipid ultrananodomains. *Biophysical Journal* 109(8), pp. 1630–1638.

Pelkmans, L. and Helenius, A. 2002. Endocytosis via caveolae. *Traffic* 3(5), pp. 311–320.

Pelkmans, L. and Zerial, M. 2005. Kinase-regulated quantal assemblies and kiss-and-run recycling of caveolae. Nature 436(7047), pp. 128–133.

Peter, B.J., Kent, H.M., Mills, I.G., et al. 2004. BAR domains as sensors of membrane curvature: the amphiphysin BAR structure. *Science* 303(5657), pp. 495–499.

Pettitt, T.R. 2009. Lipidomic analysis of phospholipids and related structures by liquid chromatography-mass spectrometry. *Methods in Molecular Biology* 462, pp. 25–41.

Pham, T.H., Zaeem, M., Fillier, T.A., et al. 2019. Targeting Modified Lipids during Routine Lipidomics Analysis using HILIC and C30 Reverse Phase Liquid Chromatography coupled to Mass Spectrometry. *Scientific reports* 9(1), p. 5048.

Pike, L.J. 2003. Lipid rafts: bringing order to chaos. *Journal of Lipid Research* 44(4), pp. 655–667.

Pike, L.J., Han, X., and Gross, R.W. (2005). Epidermal growth factor receptors are localized to lipid rafts that contain a balance of inner and outer leaflet lipids: a shotgun lipidomics study. J. Biol. Chem. 280, 26796–26804.

Pokorny, A., Kilelee, E.M., Wu, D. and Almeida, P.F.F. 2008. The activity of the amphipathic peptide delta-lysin correlates with phospholipid acyl chain structure and bilayer elastic properties. *Biophysical Journal* 95(10), pp. 4748–4755.

Prinz, W.A. and Hinshaw, J.E. 2009. Membrane-bending proteins. *Critical Reviews in Biochemistry and Molecular Biology* 44(5), pp. 278–291.

Pylypenko, O., Lundmark, R., Rasmuson, E., Carlsson, S.R. and Rak, A. 2007. The PX-BAR membrane-remodeling unit of sorting nexin 9. *The EMBO Journal* 26(22), pp. 4788–4800.

Qualmann, B. and Kelly, R.B. 2000. Syndapin isoforms participate in receptor-mediated endocytosis and actin organization. *The Journal of Cell Biology* 148(5), pp. 1047–1062.

Qualmann, B., Koch, D. and Kessels, M.M. 2011. Let's go bananas: revisiting the endocytic BAR code. *The EMBO Journal* 30(17), pp. 3501–3515.

Rao, Y. and Haucke, V. 2011. Membrane shaping by the Bin/amphiphysin/Rvs (BAR) domain protein superfamily. *Cellular and Molecular Life Sciences* 68(24), pp. 3983–3993.

Rao, Y., Ma, Q., Vahedi-Faridi, A., et al. 2010. Molecular basis for SH3 domain regulation of F-BAR-mediated membrane deformation. *Proceedings of the National Academy of Sciences of the United States of America* 107(18), pp. 8213–8218.

Razani, B., Woodman, S.E. and Lisanti, M.P. 2002. Caveolae: from cell biology to animal physiology. *Pharmacological Reviews* 54(3), pp. 431–467.

Rosenhouse-Dantsker, A. 2017. Insights into the molecular requirements for cholesterol binding to ion channels. *Current topics in membranes* 80, pp. 187–208.

Rouser, G., Kritchevsky, G., Heller, D. et al. J Am Oil Chem Soc (1963) 40: 425. https://doi.org/10.1007/BF02632842

Safari, F. and Suetsugu, S. 2012. The BAR Domain Superfamily Proteins from Subcellular Structures to Human Diseases. *Membranes* 2(1), pp. 91–117.

Salzer, U., Kostan, J. and Djinović-Carugo, K. 2017. Deciphering the BAR code of membrane modulators. *Cellular and Molecular Life Sciences* 74(13), pp. 2413–2438.

Sanchez, S.A., Tricerri, M.A. and Gratton, E. 2012. Laurdan generalized polarization fluctuations measures membrane packing micro-heterogeneity in vivo. *Proceedings of the National Academy of Sciences of the United States of America* 109(19), pp. 7314–7319.

Scita, G., Confalonieri, S., Lappalainen, P. and Suetsugu, S. 2008. IRSp53: crossing the road of membrane and actin dynamics in the formation of membrane protrusions. *Trends in Cell Biology* 18(2), pp. 52–60.

Seemann, E., Sun, M., Krueger, S., et al. 2017. Deciphering caveolar functions by syndapin III KO-mediated impairment of caveolar invagination. *eLife* 6.

Senju, Y., Itoh, Y., Takano, K., Hamada, S. and Suetsugu, S. 2011. Essential role of PACSIN2/syndapin-II in caveolae membrane sculpting. *Journal of Cell Science* 124(Pt 12), pp. 2032–2040.

Senju, Y., Rosenbaum, E., Shah, C., et al. 2015. Phosphorylation of PACSIN2 by protein kinase C triggers the removal of caveolae from the plasma membrane. *Journal of Cell Science* 128(15), pp. 2766–2780.

Senju, Y. and Suetsugu, S. 2015. Possible regulation of caveolar endocytosis and flattening by phosphorylation of F-BAR domain protein PACSIN2/Syndapin II. *Bioarchitecture* 5(5–6), pp. 70–77.

Shibata, Y., Hu, J., Kozlov, M.M. and Rapoport, T.A. 2009. Mechanisms shaping the membranes of cellular organelles. *Annual Review of Cell and Developmental Biology* 25, pp. 329–354.

Shimada, A., Niwa, H., Tsujita, K., et al. 2007. Curved EFC/F-BAR-domain dimers are joined end to end into a filament for membrane invagination in endocytosis. *Cell* 129(4), pp. 761–772.

Shimada, A., Takano, K., Shirouzu, M., et al. 2010. Mapping of the basic amino-acid residues responsible for tubulation and cellular protrusion by the EFC/F-BAR domain of pacsin2/Syndapin II. *FEBS Letters* 584(6), pp. 1111–1118.

Shoemaker, S.D. and Vanderlick, T.K. 2002. Stress-Induced Leakage from Phospholipid Vesicles: Effect of Membrane Composition. *Industrial & engineering chemistry research* 41(3), pp. 324–329.

Simunovic, M., Srivastava, A. and Voth, G.A. 2013. Linear aggregation of proteins on the membrane as a prelude to membrane remodeling. *Proceedings of the National Academy of Sciences of the United States of America* 110(51), pp. 20396–20401.

Sinha, B., Köster, D., Ruez, R., et al. 2011. Cells respond to mechanical stress by rapid disassembly of caveolae. *Cell* 144(3), pp. 402–413.

Skotland, T. and Sandvig, K. 2019. The role of PS 18:0/18:1 in membrane function. *Nature Communications* 10(1), p. 2752.

Smart, E.J., Graf, G.A., McNiven, M.A., et al. 1999. Caveolins, liquid-ordered domains, and signal transduction. *Molecular and Cellular Biology* 19(11), pp. 7289–7304.

Suetsugu, S. and Gautreau, A. 2012. Synergistic BAR-NPF interactions in actin-driven membrane remodeling. *Trends in Cell Biology* 22(3), pp. 141–150.

Suetsugu, S., Kurisu, S. and Takenawa, T. 2014. Dynamic shaping of cellular membranes by phospholipids and membrane-deforming proteins. *Physiological Reviews* 94(4), pp. 1219–1248.

Suetsugu, S., Toyooka, K. and Senju, Y. 2010. Subcellular membrane curvature mediated by the BAR domain superfamily proteins. *Seminars in Cell & Developmental Biology* 21(4), pp. 340–349.

Tachikawa, M., Morone, N., Senju, Y., et al. 2017. Measurement of caveolin-1 densities in the cell membrane for quantification of caveolar deformation after exposure to hypotonic membrane tension. *Scientific reports* 7(1), p. 7794.

Takano, K., Toyooka, K. and Suetsugu, S. 2008. EFC/F-BAR proteins and the N-WASP-WIP complex induce membrane curvature-dependent actin polymerization. *The EMBO Journal* 27(21), pp. 2817–2828.

Vedaraman, N., Brunner, G., Srinivasa kannan, C., Muralidharan, C., Rao, P.G. and Raghavan, K.V. 2004. Extraction of cholesterol from cattle brain using supercritical carbon dioxide. The Journal of supercritical fluids 32(1–3), pp. 231–242.

Wang, Q., Navarro, M.V.A.S., Peng, G., et al. 2009. Molecular mechanism of membrane constriction and tubulation mediated by the F-BAR protein Pacsin/Syndapin. *Proceedings of the National Academy of Sciences of the United States of America* 106(31), pp. 12700–12705.

Williams, T.M. and Lisanti, M.P. 2004. The caveolin proteins. *Genome Biology* 5(3), p. 214.

Yang, G., Xu, H., Li, Z. and Li, F. 2014. Interactions of caveolin-1 scaffolding and intramembrane regions containing a CRAC motif with cholesterol in lipid bilayers. *Biochimica et Biophysica Acta* 1838(10), pp. 2588–2599.

Yang, Y., Lee, M. and Fairn, G.D. 2018. Phospholipid subcellular localization and dynamics. *The Journal of Biological Chemistry* 293(17), pp. 6230–6240.

Zeghari, N., Younsi, M., Meyer, L., Donner, M., Drouin, P. and Ziegler, O. 2000. Adipocyte and erythrocyte plasma membrane phospholipid composition and hyperinsulinemia: a study in nondiabetic and diabetic obese women. *International Journal of Obesity and Related Metabolic Disorders* 24(12), pp. 1600–1607.

Zhang, Y.-L., Frangos, J.A. and Chachisvilis, M. 2006. Laurdan fluorescence senses mechanical strain in the lipid bilayer membrane. *Biochemical and Biophysical Research Communications* 347(3), pp. 838–841.

Zhao, H. and Kinnunen, P.K.J. 2002. Binding of the antimicrobial peptide temporin L to liposomes assessed by Trp fluorescence. *The Journal of Biological Chemistry* 277(28), pp. 25170–25177.

Zhao, J., Wu, J., Heberle, F.A., et al. 2007. Phase studies of model biomembranes: complex behavior of DSPC/DOPC/cholesterol. *Biochimica et Biophysica Acta* 1768(11), pp. 2764–2776.

Zhao, Y.-Y., Liu, Y., Stan, R.-V., et al. 2002. Defects in caveolin-1 cause dilated cardiomyopathy and pulmonary hypertension in knockout mice. *Proceedings of the National Academy of Sciences of the United States of America* 99(17), pp. 11375–11380.

Zimmerberg, J. and Kozlov, M.M. 2006. How proteins produce cellular membrane curvature. *Nature Reviews. Molecular Cell Biology* 7(1), pp. 9–19.